3 (2026) 100214

Contents lists available at ScienceDirect

The EANM Journal

journal homepage: www.sciencedirect.com/journal/the-eanm-journal

Joint EANM/SNMMI recommendations on the use of Tau PET imaging in Alzheimer's disease

A B S T R A C T

The purpose of these recommendations is to assist nuclear medicine practitioners in recommending, performing, interpreting, and reporting tau PET imaging of the brain (tau PET) in patients with cognitive impairment suspected of Alzheimer's disease (AD). Tau pathology represents a central hallmark of AD and an important biomarker within the biological AT(N) framework, where tau PET imaging enables in vivo assessment for diagnostic evaluation, prognosis, and patient stratification. These joint recommendations from the European Association of Nuclear Medicine (EANM) and the Society of Nuclear Medicine and Molecular Imaging (SNMMI) provide a framework to support the clinical and research use of tau PET imaging. The document covers the currently approved radiotracer [^{18}F]flortaucipir as well as several widely used next-generation tau PET radiotracers. It provides guidance on appropriate clinical indications, patient preparation, image acquisition, visual interpretation, quantitative analysis, and standardized reporting procedures.

Particular emphasis is placed on harmonized procedures for image interpretation and quantification, including the use of standardized uptake value ratios (SUVRs), appropriate reference regions, and emerging harmonization approaches that enable comparison of quantitative measures across radiotracers and imaging centers. Standardized imaging procedures are essential to ensure robust and reproducible measurements and to facilitate the integration of tau PET into clinical workflows and multicenter studies.

Preamble

The European Association of Nuclear Medicine (EANM) is a professional, non-profit medical association dedicated to facilitating global communication between individuals striving for clinical and research excellence in nuclear medicine. The EANM was founded in 1985. The Society of Nuclear Medicine and Molecular Imaging (SNMMI) is an international scientific and professional organization founded in 1954 to advance the science, technology, and practice of nuclear medicine. The EANM and the SNMMI bring together physicians, technologists, medical physicists, radiochemists and - pharmacists as well as scientists involved in nuclear medicine research and practice.

These guidelines are an educational tool designed to assist practitioners in providing appropriate nuclear medicine care to patients and to advance the science of nuclear medicine, ultimately improving the quality of care worldwide. While they are intended to guide clinical practice, they are not inflexible rules or mandatory requirements, nor should they be used to establish a legal standard of care. For these reasons, the EANM and the SNMMI caution against the use of these guidelines in litigation where a practitioner's clinical decisions are being questioned.

The EANM and the SNMMI regularly produce new guidelines and reviews existing guidelines for revision or renewal, usually on their fifth anniversary. Each guideline represents a carefully considered policy statement by the EANM and the SNMMI, developed through an extensive consensus process and subject to extensive peer review. The EANM and the SNMMI recognise that the safe and effective use of diagnostic and therapeutic nuclear medicine requires specific training, skills and techniques, as described in each document. Reproduction or modification of these guidelines by entities not directly involved in the provision of these services is strictly forbidden.

The ultimate judgment as to the appropriateness of a particular procedure or course of action must be made by the (medical) professionals, considering the individual circumstances of each case. Consequently, a decision to deviate from the guidelines should not in itself be considered a deviation from the standard of care. On the contrary, a conscientious practitioner may responsibly choose an alternative approach if, in his or her reasonable judgement, such an approach is indicated by the patient's condition, the limitations of available resources, or advances in knowledge or technology since the guidelines were published.

The practice of medicine involves not only the science but also the art of preventing, diagnosing, alleviating and treating of disease.

Because of the diversity and complexity of human disease, it is not always possible to make the most accurate diagnosis or to predict with certainty a particular response to treatment. Therefore, it should be recognized that following these guidelines does not guarantee an accurate diagnosis or a successful outcome.

The reasonable expectation is that the practitioner will follow a reasonable course of action based on current knowledge, available resources and the needs of the patient, with the aim of providing effective and safe medical care. The sole purpose of these guidelines is to assist practitioners in achieving this goal.

1. Introduction

Aggregation of hyperphosphorylated tau protein is a recognized hallmark of Alzheimer's disease (AD) [1] and emerged as one major pillar of the biological AT(N) classification of AD [2–4]. Tau aggregates into distinct forms, from early pretangles to mature neurofibrillary tangles (NFTs) and ultimately ghost tangles [5]. Tau accumulation follows a predictable spatial progression as outlined by Braak staging [6].

https://doi.org/10.1016/j.eanmj.2026.100214
Received 30 January 2026; Received in revised form 5 March 2026; Accepted 6 March 2026
Available online 30 March 2026

Histological analyses have revealed a complex interplay between tau isoforms, particularly the three-repeat (3R) and four-repeat (4R) variants [7]. Recent findings indicate that tau pathology evolves through an isoform shift, from an initial predominance of 4R tau in early pretangles to increasing levels of 3R tau in mature NFTs and ghost tangles [8]. The regional progression of neurofibrillary pathology is increasingly viewed through a circuit-oriented lens, supported by evidence that tau misfolding can propagate along neural networks in a prion-like manner [9,10]. However, the precise mechanisms of this spread remain to be fully elucidated. In parallel, PET imaging has emerged as a critical tool for in vivo visualization of tau deposits, which provided valuable correlations between PET signal and histopathological Braak stages [11,12]. Next-generation radiotracers demonstrated a high affinity for mixed 3/4R tau in AD and fibrillar tau in the brain of patients with AD correlates closely with clinical severity [13] while its topological distribution defines disease subtypes of AD [14]. Since tau PET predicted clinical progression by a positive visual read [15], it is increasingly entering clinical routine workflows. Furthermore, a recent multicenter evaluation of over 12.000 individuals uncovered the dependency of tau-positivity based on age, sex, amyloid-β biomarkers, and APOE4 status [16]. Altogether, this highlights the value of the assessment of tau as an objective biomarker of disease progression in AD, and therefore, standardized procedures are highly demanded to ensure robustness of the methodology.

2. Goals

The goal of this recommendation is to assist nuclear medicine practitioners in recommending, performing, interpreting, and reporting the results of brain PET imaging that depicts tau aggregation in the brain (referred to as tau PET hereafter). This recommendation covers [^{18}F]Flortaucipir as the only currently approved tau PET radiotracer as well as several promising next generation tau PET since they are already commonly used by the community.

3. Common clinical indications

Updated appropriate-use criteria for tau PET have been published recently by the SNMMI and Alzheimer's Association joint task force [17,18]. The appropriate-use criteria emphasize that tau PET is currently most likely to be helpful i) when the patient presents with MCI or dementia syndrome who are younger than 65 years and in whom AD pathology is suspected, ii) when the patient presents with atypical features such as non-amnestic presentation, rapid or slow progression, or etiologically mixed presentation. Other appropriate indications include iii) determining the prognosis of patients presenting with MCI due to clinically suspected AD pathology, iv) determining the prognosis of patients presenting with dementia due to clinically suspected AD pathology, and v) determining eligibility for treatment with an approved amyloid-targeting therapy.

Furthermore, before considering tau PET it needs to be ensured that AD is considered a reasonable differential diagnosis of the cognitive impairment, but the etiology remains uncertain after a comprehensive evaluation by a dementia expert. Dementia experts are defined as physicians trained and board-certified in neurology, psychiatry, or geriatric medicine who devote a substantial proportion (>25%) of patient contact time to the evaluation and care of adults with acquired cognitive impairment or dementia, including probable or suspected AD [19]. Furthermore, as a second prerequisite, knowledge of the presence or absence of tau pathology is expected to help establish the etiology of impairment and alter clinical management.

Due to the predominant use of tau PET in research settings, several scenarios with uncertain value exist [17,18] and include i) patients presenting with MCI or dementia syndrome that is often consistent with AD pathology (amnestic presentation) with onset at 65 years or older, ii) determination of disease severity or tracking of disease progression in patients with an established biomarker-supported diagnosis of MCI or dementia due to AD pathology, iii) patients presenting with prodromal Lewy body disease or DLB, iv) patients with MCI or dementia with recent CSF biomarker results that are conclusive (whether consistent or not consistent with underlying AD pathology), v) patients with MCI or dementia with equivocal or inconclusive results on recent CSF biomarkers or on structural imaging with MRI and CT, vi) monitoring response among patients who have received an approved amyloid-targeting therapy. Further health services research is necessary to determine effective clinical use of tau PET in these conditions.

The use of tau PET is considered inappropriate when there is nonmedical usage (e.g., legal, insurance coverage, or employment screening) or in lieu of genotyping for suspected autosomal dominant mutation carriers.

This recommendation is primarily intended for AD tau PET imaging but some of the discussed radiotracers provide distinct topological patterns in primary tauopathies (i.e. signal in the basal ganglia), which may come to attention of practitioners. These details are not discussed in greater detail since no radiotracers are approved for non-AD indications, but they can be found in the specific chapters of the respective radiotracers on demand.

4. Procedure/specifications of the examination

By the end of 2024, [^{18}F]Flortaucipir was approved by the U.S. Food and Drug Administration (FDA, 5/2020) and the European Medicines Agency (EMA, 8/2024) for tau PET examinations. Several next-generation tau PET radiotracers have been developed, and three of them are currently in or have completed Phase III trials ([^{18}F]MK-6240, [^{18}F]PI-2620, [^{18}F]Florzolotau; for details, see Table 1). Required qualifications and responsibilities of personnel as well as information with regard to study request and patient preparation are provided in the **Supplement**.

5. Radiopharmaceuticals and image acquisition

The following chapter provides an overview of characteristics of frequently used tau PET radiotracers (Table 1, Fig. 1), including appropriate administered activities and time windows for imaging, off-target sources, and major studies conducted with these compounds. The most important details for practitioners to implement tau PET imaging in molecular imaging units are summarized in Table 2, whereas additional details and relevant literature can be found in the following chapters on the specific radiotracer on demand. Standardized uptake value ratios (SUVRs) with an inferior cerebellar reference region represent the commonly used parameter to measure regional binding values of tau PET radiotracers as a simplified semi-ratio.

The imaging protocols mentioned below focus solely on the time-point recommended for their ability to measure tau pathology, but it is important to remind the reader that some groups acquired images immediately after injection (early frames or dual-time acquisitions) as proxy of cerebral brain perfusion and metabolism and thus of neurodegeneration using [^{18}F]Flortaucipir, [^{18}F]MK-6240 or [^{18}F]PI-2620 [27–30]. As the experience in the literature is still limited a specific

Table 1
Tau PET radiotracers with high clinical or investigational use in 2025. [1][^{18}F]AV1451; [2][^{18}F]APN-1607.

Tau radiotracer	Development status
[^{18}F]Flortaucipir[1]	FDA (05/2020) and EMA (08/2024) approved (TAUVID™)
[^{18}F]Florzolotau[2]	Investigational, one Phase III study completed (NCT05542953)
[^{18}F]GTP1	Investigational
[^{18}F]MK-6240	NDA submitted; under review
[^{18}F]PI-2620	Investigational, Phase III study ongoing (NCT05641688)
[^{18}F]RO-948	Investigational

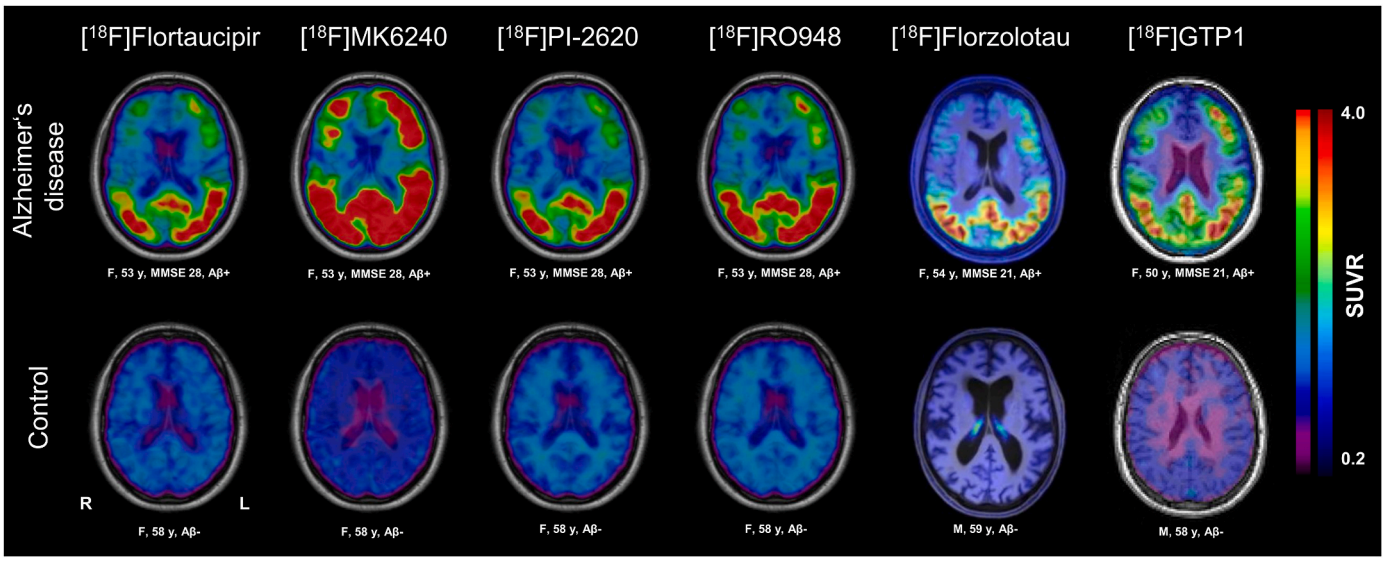

Fig. 1. Representative images of discussed tau PET radiotracers for Alzheimer's disease (AD) and controls. Please note that [^{18}F]Flortaucipir, [^{18}F]MK-6240, [^{18}F]PI-2620, and [^{18}F]RO948 images are derived from the same individuals of the HEAD study [20], adjusted to the left color bar. The right color bar applies to [^{18}F]Florzolotau, [^{18}F]GTP1.

Table 2
Overview on relevant parameters needed for installing tau PET imaging in molecular imaging units. *Assumes 2 hr voiding interval. **Assumes 1.5 hr voiding interval. p.i. = post injection. AD = Alzheimer's disease. PSP = Progressive supranuclear palsy.

Tau radiotracer	Activity [MBq]	Scan start time [min p.i.]	Scan duration [min]	Effective dose [μSv/MBq]	"Critical" organ
[^{18}F]Flortaucipir	370	80	20	23.5 [21]	Large intestinal wall, small intestine, and liver.
[^{18}F]Florzolotau	185 - 370	90	20	19.7 - 34.9 [22]	Right colon, gallbladder
[^{18}F]GTP1	250	60	30	28.6* [23]	Gallbladder, urinary bladder*, liver, kidneys
[^{18}F]MK-6240	180 - 250	90	20	26.8 - 29.4 [24]	Gallbladder and urinary bladder
[^{18}F]PI-2620	185	45 min (AD) 60 min dynamic (PSP) or 20 min or 30 min static scan	30 min (AD) 60 min dynamic (PSP) or 20-30 min static scan	33.1 - 33.3** [25]	Right colon (ascending + first half of transversal colon)
[^{18}F]RO-948	370	60-70	20-30	15.0 [26]	Gallbladder

recommendation cannot be provided on the use of early perfusion imaging. However, there is agreement about the fact that these additional images provide complementary information as compared to the standard late frames and should be acquired whenever possible.

[^{18}F]Flortaucipir: [^{18}F]Flortaucipir (also known as [^{18}F]AV-1451 or T807), marketed as Tauvid, is an [^{18}F]-labeled PET radioligand that selectively binds to aggregated tau in neurofibrillary tangles (NFTs) developed by Avid, a wholly-owned subsidiary of Eli Lilly and Company. It is the first PET radiotracer specifically targeting tau pathology to receive approval from both the FDA and EMA. According to its label for clinical use, [^{18}F]Flortaucipir is indicated for estimating the density and distribution of aggregated tau NFTs in the brains of adults with cognitive impairment being evaluated for AD [31,32]. The recommended activity is 370 MBq (10 mCi), administered via intravenous injection. Image acquisition should begin approximately 80 min post injection, with a recommended scan duration of about 20 min. In clinical practice, evaluation of a [^{18}F]Flortaucipir PET scan is performed using a standardized visual interpretation method [11].

[^{18}F]Flortaucipir was designed to selectively target tau, but it also binds to certain off-target sites, which can produce signal in regions without tau NFTs [33]. Notably, monoamine oxidase enzymes (MAO-B) have high in vitro affinity for [^{18}F]Flortaucipir [34]. However, MAO-B binding in vivo appears to be minimal [35,36]. More prominent off-target binding is seen in tissues rich in melanin or iron. For example, the midbrain (substantia nigra) and locus coeruleus contain neuromelanin, and the meninges harbor melanocytes; [^{18}F]Flortaucipir shows uptake in these regions even in the absence of tau [37–39]. Similarly, iron-rich areas like the basal ganglia (e.g. globus pallidus) can show non-specific radiotracer retention [40]. The choroid plexus often displays [^{18}F]Flortaucipir binding as well, possibly due to calcifications or melanin in choroid plexus cells [38]. These off-target signals can complicate quantitative assessments of [^{18}F]Flortaucipir; for instance, choroid plexus uptake adjacent to the hippocampus may spill signal into that area and mimic mesial temporal lobe binding [41], justifying exclusion of the hippocampus from quantitative analyses. Although [^{18}F]Flortaucipir generally shows low non-specific background uptake in the cortex, it is important to be aware of off-target binding in areas such as the midbrain, basal ganglia, choroid plexus, and meninges to avoid misinterpretation during image analysis. With appropriate training, off-target binding does not typically complicate visual interpretation of [^{18}F]Flortaucipir PET scans.

[^{18}F]Flortaucipir has been extensively validated against postmortem pathology. A pivotal Phase III PET-to-autopsy study (A16) [11] enrolled terminally ill patients who underwent a [^{18}F]Flortaucipir PET scan and

demonstrated that it could predict the presence of advanced tau pathology at autopsy with high accuracy. In that study, [^{18}F]Flortaucipir's visual interpretation method showed sufficient sensitivity and specificity (94.4% and 80.8% respectively for a majority read) for detecting advanced Braak stage V/VI tau pathology, meeting the performance criteria required for FDA approval. The ability of [^{18}F]Flortaucipir to reliably identify Braak stage V/VI tau pathology has since been confirmed in additional PET-to-autopsy studies [42–45]. More recently, a clinically applicable visual interpretation method has been proposed in the I7E-AV-A26 study, enabling the classification of [^{18}F]Flortaucipir PET–positive individuals into groups with high versus non-high tau burden [46].

In therapeutic trials, [^{18}F]Flortaucipir PET has been used as both an inclusion biomarker and secondary endpoint. It was used to identify individuals with low to medium tau burden for enrollment in the Phase II and Phase III trials of the anti-amyloid therapy donanemab, both of which demonstrated positive results [47,48]. Importantly, data from the Phase III study indicated that lower baseline tau burden, as measured with [^{18}F]Flortaucipir PET, was associated with greater clinical benefit from the treatment [47]. In addition to the donanemab trials, [^{18}F]Flortaucipir PET has been employed as an outcome measure in several other clinical studies, including trials targeting amyloid pathology (e.g., the A4 study [49]) and tau pathology (e.g. PERISCOPE-ALZ [50] and PROSPECT-ALZ [51]).

[^{18}F]Florzolotau: [^{18}F]Florzolotau, also known as [^{18}F]PM-PBB3 or [^{18}F]APN-1607, is a second-generation tau PET radiotracer developed by APRINOIA Therapeutics, which shows high affinity (K_D = 7.6 nM) and calculated binding potential (B_{max}/K_D = 752.7) to 3R/4R tau in AD tissue [52]. *In vitro*, this radiotracer did not effectively bind to β-amyloid deposits in AD homogenates, and there was only minimal displacement of tau binding by MAO-A or -B inhibitors [52]. 185 – 370 MBq of this radiotracer are administered to the patients, and (pseudo)equilibrium 20 min PET scans starting 90 min post injection (p.i.) are typically acquired [52]. Apart from imaging AD tau, [^{18}F]Florzolotau is reported to owe potential to image 4R-tau as found in progressive supranuclear palsy (PSP) or corticobasal degeneration (CBD), and 3R-tau as found in certain cases with frontotemporal lobar degeneration [52–55]. [^{18}F]Florzolotau binding in the AD spectrum follows the topology of Braak's neurofibrillary tangle stages [52]. Based on automated image analysis, [^{18}F]Florzolotau was able to discriminate patients with dementia from AD from healthy controls with high accuracy (area under the receiver-operating characteristic curve (AUC_{ROC}) = 0.99) [56]. Similar findings were reported for patients with PSP (AUC = 1.0) and patients with non-AD neurodegenerative diseases (AUC = 0.95) [46,45]. Individual cases with ante-mortem [^{18}F]Florzolotau PET to autopsy were published for PSP [57], Pick's disease [58], and CBD/PSP [52,59].

[^{18}F]GTP1: [^{18}F]Genentec tau probe 1 ([^{18}F]GTP1) is a second-generation tau PET radiotracer developed by Genentec. The molecule is the deuterated form of the T808 chemical backbone [23]. In vitro binding affinity of [^{18}F]GTP1 to 3/4R tau is high (Kd 10.8 ± 1.1 nM) with negligible affinity to MAO-B or β-amyloid [23]. Typically, 30 min PET scans are acquired 60 min p.i. after administration of 250 MBq of this radiotracer. First-in-human [^{18}F]GTP1 PET data in patients with AD and healthy controls showed relevant retention in AD in cortical regions consistent with 3R/4R tau deposition [23]. For quantification, the cerebellar grey matter was employed as reference region [60]. It was also demonstrated that standardized uptake value ratios (SUVRs) obtained during the above static time-window correlate with quantitative retention parameters as obtained by kinetic modeling [60]. Test-retest variability of SUVRs in the 60-90 min p.i. window was 3.7% [23]. In Phase II studies in subjects of the AD spectrum, cognitive impairment was correlated with [^{18}F]GTP1 retention, and greater baseline [^{18}F]GTP1 PET signals were associated with faster rates of subsequent cognitive decline [60–62]. Head-to-head in vivo PET vs. post mortem histopathology comparisons are not yet published for this radiotracer. There is, however, a head-to-head radiotracer comparison study available indicating that [^{18}F]GTP1 exhibits similar uptake patterns to other tau PET radiotracers ([^{18}F]PI-2620 and [^{18}F]MK-6240) in AD patients [63]. Tau PET imaging using [^{18}F]GTP1 is being incorporated into several therapeutic trials.

[^{18}F]MK-6240: [^{18}F]MK-6240 (also known as [^{18}F]Florquinitau) is a second-generation PET radiotracer developed by Merck and now owned by Lantheus. The [^{18}F]MK-6240 binding pocket is found within tau fibrils and seeds [64]. Typically, 180 - 250 MBq of this radiotracer is administered, and PET scans are acquired for 20 minutes for this radiotracer. Initially, 70-90 min p.i. has been proposed, a time-window in which the SUVRs correlate with kinetic modeling-based radiotracer retention readouts [65,66]. It was observed that this radiotracer reached equilibrium at 60 min p.i. in low-binding regions, whereas medium- and high-binding regions required approximately 90 minutes to reach equilibrium, prompting the recommendation of a 90-110 p.i. window to ensure accurate quantification [67]. Most [^{18}F]MK-6240 studies used the cerebellar grey matter as reference region for quantification [66,24,68,69]. A test-retest study employing low (165 MBq) and high (300 MBq) radiotracer activities did not find significant SUVR differences [69]. Short-term and long-term test-retest variability of SUVRs as obtained by [^{18}F]MK-6240 was reported as 6% [69] and 3% [70]. With regard to off-target binding of this radiotracer, the ethmoid, straight and transverse sinus, clivus, sphenotemporal buttress, pineal gland, substantia nigra, superior anterior vermis, superior cerebellum, and especially the meninges are reported [65]. For this radiotracer, so far, two cases of in vivo PET imaging vs. post mortem histopathology comparisons have been published demonstrating a strong correlation between the PET findings and AT8 immunostaining for tau aggregates [71]. However, [^{18}F]MK-6240 post-mortem validation data are limited.

[^{18}F]PI-2620: [^{18}F]PI-2620 is a second-generation tau PET radiotracer which is currently developed by Life Molecular Imaging, now a Lantheus company, to gain approval for imaging both 3R/4R-tau in AD and 4R tau in PSP and other tauopathies. Typically, 185 MBq of this radiotracer are administered to the patient. First-in-human data in AD showed that after 40 min p.i., SUVRs reach an apparent steady state, and that respective static SUVRs correlate with kinetic modeling data on radiotracer binding [72]. Robust imaging windows to capture AD tau were reported between 30 and 75 min p.i. [73], whereas dynamic imaging in 0-60 min or 0-40 min intervals provided highest contrast in patients with 4R tauopathies [74]. The radiotracer was also reported to exhibit acceptable radiation exposure, low test-retest variability, and high effects sizes in the discrimination between patients with AD and healthy controls [25,75,76]. Apart from imaging AD tau, [^{18}F]PI-2620 indicated potential to image 4R-tau as found in PSP [77] and CBD [78]. Off-target binding of this radiotracer was found to be lower than that of first-generation radiotracers, especially in the basal ganglia region [79], which is of particular relevance with regard to detecting 4R-tauopathies such as PSP, showing tau-aggregation precisely in these regions. Other off-target sources were reported for hemorrhagic lesions, retinal pigment epithelium, and neuromelanin-containing neurons of the substantia nigra [80], as well as leptomenigeal melanocytes [81]. Preliminary evidence was also published pointing to the potential of this radiotracer to image AD tau aggregates in all six Braak stage brain areas [82]. Initial longitudinal PET data demonstrated that this radiotracer has likewise potential to track tauopathy progression in AD over time [83,84]. [^{18}F]PI-2620 PET to autopsy correlations were reported for limited patients with 4R tauopathies [85], whereas a PET to autopsy trial in AD is ongoing.

[^{18}F]RO-948: [^{18}F]RO-948 (previously known as RO6958948) is a second-generation tau PET radiotracer developed by Roche specifically to image tau pathology in AD [26]. Compared to earlier radiotracers of this family, [^{18}F]RO-948 offers improved specificity for aggregated tau proteins, particularly the paired helical filaments characteristic of AD in the medial temporal lobe, along with better kinetic properties [33,26,86]. Imaging with this radiotracer has typically been performed using a activity of 370 MBq [87,88] and an acquisition window starting at 60-70

min p.i. and finishing at 90 min p.i., a window in which the SUVRs reach an equilibrium [89]. Quantitative analysis approaches with [^{18}F]RO-948 typically involve SUVR calculations using the inferior cerebellar cortex as the reference region. More recently, individualized ROI methods, tailoring regions based on participant-specific radiotracer retention patterns, have been introduced, offering improved sensitivity to longitudinal change and reduced sample size requirements compared to group-level ROIs [90]. Main regions of off-target binding of this radiotracer are the basal ganglia, white matter, thalamus, substantia nigra, choroid plexus, skull and meninges [86,88,91]. [^{18}F]RO-948 has low binding to MAO-B [92]. [^{18}F]RO-948 has been evaluated in several research observational studies, including the BioFINDER study [87,93] and the FACEHBI cohort [88]. These studies have explored its ability to detect early tau accumulation and to monitor longitudinal changes over time, demonstrating its value for early diagnosis and tracking disease progression in AD. To date, [^{18}F]RO-948 has not been used as an outcome measure in clinical trials and no ante mortem PET to autopsy data were published for tauopathy brains.

5.1. Visual image interpretation

The methods for visual image interpretation of tau PET scans are still in the process of optimization and the stage of this process differs per radiotracer. Therefore, this procedure recommendation briefly reviews the current status for the visual interpretation methods for the most commonly used tau PET radiotracers. Before interpretation of the images, it is important that the images are critically examined for the presence of movement or attenuation artifacts. The most important details for practitioners to visually assess tau PET images are summarized in Table 3, whereas details and relevant literature can be found in the following chapters on the specific radiotracer. Whereas the visual image interpretation methods that are assessed for the tau PET radiotracers still differ, there are several general items that are of importance for all:

Color scale: almost all visual read methods that have been proposed recommend a high-contrast color scale, such as rainbow scale. More specifically, the FDA/EMA approved method for [^{18}F]Flortaucipir advises the selection of a color scale for image display that has a rapid transition between two distinct colors in the general range of 25% to 60% of maximum intensity (Fig. 2). The rapid transition between colors enhances the sensitivity for demonstrating increased binding.

Reference region: Several methods propose to normalize the intensity to the cerebellum, either whole cerebellum or cerebellar grey matter, to enhance the sensitivity. This is recommended for both [^{18}F]Flortaucipir and [^{18}F]MK-6240, and this approach has also improved sensitivity for [^{18}F]PI-2620. Hence, scaling based on cerebellar activity as reference should be considered and further assessed for all tau PET radiotracers.

Staging: Since the distribution of increased binding of tau PET radiotracers is strongly associated with the Braak stages, several studies propose to add information on staging and binding pattern in the report. Commonly used categories are 'no increased binding', intermediate binding and high binding to rate the intensity of radiotracer signal. Furthermore, medial temporal binding, lateral temporal/occipital binding, and parietal, precuneus binding are used to describe the spatial extent. In addition, the category non-AD pattern is regularly used to indicate that increased binding is observed, e.g. in frontal regions, but that it does not follow the typical AD pattern, suggesting that the increased binding may not be related to underlying AD tau pathology. Another suggested category to describe the binding pattern is medial temporal lobe (MTL)-sparing, in case of typical AD pattern without increased uptake in the MTL. These staging categories may also be relevant for clinical trials, as it has been shown that patients with intermediate tau load, seem to have more benefit from anti-amyloid therapy than patients with high tau load [109]. Finally, initiatives to develop a common visual read method that can be used for the different tau PET radiotracers are currently under development. Methods combining visual assessment with a semi-quantitative measure are not yet assessed but have the potential to improve diagnostic accuracy.

Differential diagnosis: Most published approaches of standardized visual reading of tau PET images focused on discrimination between tau-positive versus tau-negative findings which may not exploit the full strength of the method with regard to detection of specific patterns (i.e. differential diagnosis) and interpretation of severity (i.e. signal intensity and spatial extent). Practitioners need to be aware of typical and atypical AD patterns of tau PET signals and their distinct expression, as exemplified in Fig. 3. Furthermore, some of the radiotracers can show non-AD patterns of radiotracer uptake, such as striatal signals in 4R tauopathies or fronto-temporal signals in 3R or 4R tau-positive fronto-temporal dementia when using [^{18}F]Florzolotau and [^{18}F]PI-2620 (Fig. 3). Origins of these signals are not fully disentangled and they were not challenged in clinical trials yet. However, the practitioner needs to be aware of their occurrence, and close correlation with clinical symptomology is recommended for interpretation. As one example, [^{18}F]Flortaucipir in the left anterior temporal lobe is also observed in amyloid negative patients with semantic dementia [110], but does not appear to correspond to tau, MAO-B, or TDP-43 [111]. This phenomenon may limit the radiotracer's utility for differentiating semantic dementia from the logopenic variant of AD and further studies need to investigate if second generation radiotracers provide improved discrimination. Importantly, it has been discussed that the uptake pattern of tau PET radiotracers may not only differentiate between tau-positive and tau-negative forms of disease and between different types of tau-positive forms but also provide evidence on the β-amyloid-status [112,113]. For this reason, tau PET has also been considered to be helpful to select patients for amyloid-targeting therapies in the updated Appropriate Use Criteria. Together with the option to even discriminate different forms of tau-negative neurodegeneration based on early perfusion-patterns (as discussed above), tau PET may bear potential for integrated assessment of amyloid-, tau- and neurodegeneration status, thus serving as a universal tool for one-stop A/T/N classification. This aspect requires further investigation.

[^{18}F]Flortaucipir: [^{18}F]Flortaucipir is currently the only tau PET radiotracer with a regulatory-approved visual interpretation method, following FDA approval in 2020 and EMA approval in 2024 (https://www.accessdata.fda.gov/drugsatfda_docs/label/2024/212123s031lbl.pdf). The standardized read method relies on a binary classification: scans are considered *positive* for AD if they exhibit elevated radiotracer uptake in the posterolateral temporal, parietal, or occipital cortices, with or without involvement of the frontal lobes, patterns consistent with Braak stages IV–VI. Importantly, scans are suggested to be classified as *negative* not only if uptake is absent in these neocortical regions but also if existing uptake is restricted to the medial temporal lobes, consistent with early-stage tau pathology (Braak I–III) or age-related changes. Consequently, this reading strategy may result in classification of some scans as "tau-negative" despite showing measurable tau radiotracer retention (potentially reflecting tau-pathology). On the other hand, this visual interpretation algorithm demonstrates high inter-rater agreement (Cohen's $\kappa > 0.87$) and high sensitivity (92–100%) for detecting Braak III-level tau pathology [114,115]. Thus a "*positive*" scan is likely reflecting AD-typical tauopathy beyond the very early stages. Importantly, it has been demonstrated that mesial temporal tau pathology may in fact predict further cognitive decline particularly in amyloid-positive subjects [116]. It may therefore be discussed if instead of reporting scans with isolated mesial/anterior temporal or frontal radiotracer uptake as "tau-negative", a different terminology may be preferable, e.g. "pattern not consistent with AD-typical tauopathy beyond the very early stages" (or similar). Such interpretation of a non-AD-typical pattern would also include primary age related tauopathy (PART), which however did not translate into elevated mesial temporal [^{18}F]Flortaucipir signals [117]. Fleisher et al. [118] proposed an extended classification, further stratifying positive scans into

Table 3
Overview on clinical trials and features of visual and quantitative image interpretation.

Tau radiotracer	Phase I, II, III studies	Visual read strategy	Off target sources	Test-retest variability [%]	Effect size AD vs. HC (tau meta VOI)
[^{18}F]Flortaucipir	Phase I: NCT01992380 Phase II: NCT02016560 Phase III: NCT02516046 NCT03901092	FDA/EMA-approved; binary classification [11]	Choroid plexus, basal ganglia, thalamus, brainstem nuclei, meninges and skull, vascular or hemorrhagic lesions [38,39,41,94]	2% to 6% [95,96]	Cohen's d > 2 [97]
[^{18}F]Florzolotau	Phase II: NCT04141150 Phase III: NCT05542953 (study ongoing)	Not yet formally validated (for pragmatic approaches see: [53,98,99])	Choroid plexus, pituitary gland, putaminal uptake in multiple system atrophy [100]	Not available	Cohen's d: AD vs. Aβ- HC: 2.48 (49) AD vs. HC (Amyloid-status unknown): 1.91 [101]
[^{18}F]GTP1	Phase I: NCT02640092 NCT04394845 Phase II: NCT02640092	Not formally validated	Putamen, Pallidum, skull, meninges, choroid plexus	3.7%	Cohen's d: 1.59-2.07 [102]
[^{18}F]MK-6240	Phase I: NCT02562989 Phase II: NCT03919669	Four-class visual read approaches validated [103,104]	Neuromelanin- and melanin-containing cells Meninges, Ethmoid and transverse sinus, Clivus, sphenotemporal buttress, pineal gland, Substantia nigra, Superior anterior vermis, Superior cerebellum [65] Eyes, putamen and pallidum (Lower magnitude than other radiotracers and not visually perceptible [105])	~6% for $SUVR_{90\text{-}110}$ [69]	Cohen's d: 1.91 (mean age in AD: 71.2) [106]
[^{18}F]PI-2620	Phase I: NCT05187546 Phase II: NCT03903211 Phase III: NCT05641688 (study ongoing)	Three-class visual read method validated [107]	Venous sinus, retina, scalp, vermis, substantia nigra, meninges, leptomeningeal melanocytes, choroid plexus	4.3% (AD, average for SUVR (45-75min) across cortical regions) ICC: 0.96 (AD) [25]	Cohen's d: 3.8 (across all cortical regions analyzed) [25]
[^{18}F]RO-948	Not available	Four-class visual read approach validated [108]	Meninges, skull [86,88]	4.6% [89]	Cohen's d = 3.1 [87]

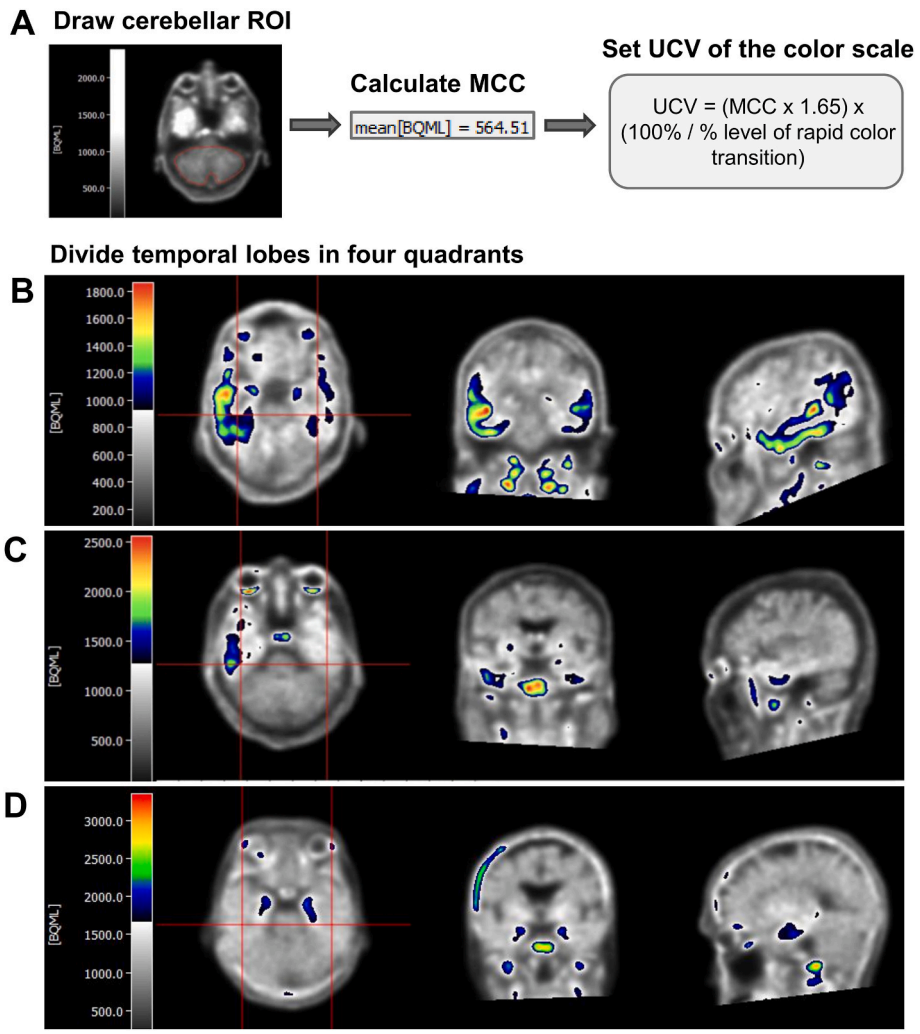

Fig. 2. Visual interpretation at a glance. [^{18}F]Flortaucipir PET scans of three study participants are illustrated using the FDA/EMA-approved visual read method [11]. (**A**) shows how a region of interest is drawn around the cerebellum in the transverse plane, where the mean cerebellar counts (MCC) are measured. After setting the upper contrast value of the color scale, using a visual threshold of 1.65 x MCC, the temporal lobes are divided into four quadrants (**B, C, D**). The images shown in (**A**) and (**B**) are from the same individual, representing an advanced positive scan (**B**). In subject (**C**) a moderate positive scan is observed, as increased intensity reaches into the posterior lateral temporal lobe. Tau PET scan (**D**) shows a negative scan, as only the mesio temporal lobe shows increased uptake. In (**B**) and (**C**) the positive category is further specified (moderate or advanced positive) adhering to Fleisher et al.

moderate and *advanced* AD tau patterns based on the topographic spread of neocortical uptake. Moderate patterns involve radiotracer retention in the posterolateral temporal or occipital cortex, while advanced patterns show additional involvement of the parietal, precuneus, or frontal cortices. This refined approach maintains high inter-rater reliability (Fleiss' $\kappa = 0.80$) and comparable sensitivity (92.3–100%) in post-mortem confirmed Braak III-level tau pathology. Additional visual rating strategies have been proposed to better capture the phenotypic spectrum of tau pathology. Sonni et al. [119] introduced a combined visual scoring framework using a global uptake score and a four-pattern classification: *negative*, *medial temporal*, *AD-like*, and *non-AD-like*. This scheme largely overlaps with Fleisher's method and has shown satisfactory intra- and inter-rater agreement ($\kappa \geq 0.71$). Mathoux et al. [120] reported on a visual read algorithm where readers assign scans a stage (I–VI) based on anatomical distribution of uptake. This approach has achieved a close alignment with neuropathological Braak staging while preserving clinical interpretability and demonstrates good inter-rater reliability across experience levels (overall $\kappa = 0.71$). Tunali et al. [46] proposed a two-step "visual stratification" method. In a first step, readers classify scans into AD vs non-AD patterns based on Fleisher's framework. In a second step, they apply a higher uptake threshold (>2.8 times the cerebellar signal) to identify individuals with high tau burden. This approach achieved high inter-rater agreement (Fleiss' $\kappa = 0.89$). All methods apply a high-contrast color scale (typically rainbow and spectre) and normalize intensity relative to the cerebellum. Areas of radiotracer retention are defined as voxels exceeding 65% above cerebellar reference activity, by estimating mean cerebellar counts or manually adjusting the color scale (see Fig. 2). To define/detect "elevated" radiotracer uptake, it is suggested according to the product information to use a threshold of 1.65 x mean uptake in the cerebellum and to adjust a multi-color scale so that it shows abrupt transition of colors at this threshold level (using a predefined formula). By applying this method, a hard/objective cutoff is defined for qualitative visual analysis, which must be reached/exceeded in order to obtain a positive scan. This distinguishes the method in particular from visual methods of evaluating β-amyloid imaging. Compared to more recent second generation tau radiotracers such as [^{18}F]MK-6240 or [^{18}F]PI-2620, [^{18}F]Flortaucipir shows greater off-target binding in regions such as the choroid plexus, which may limit the sensitivity for detecting early medial temporal uptake.

[^{18}F]Florzolotau: A visual read strategy for AD that has been formally validated in a prospective setting (with or without

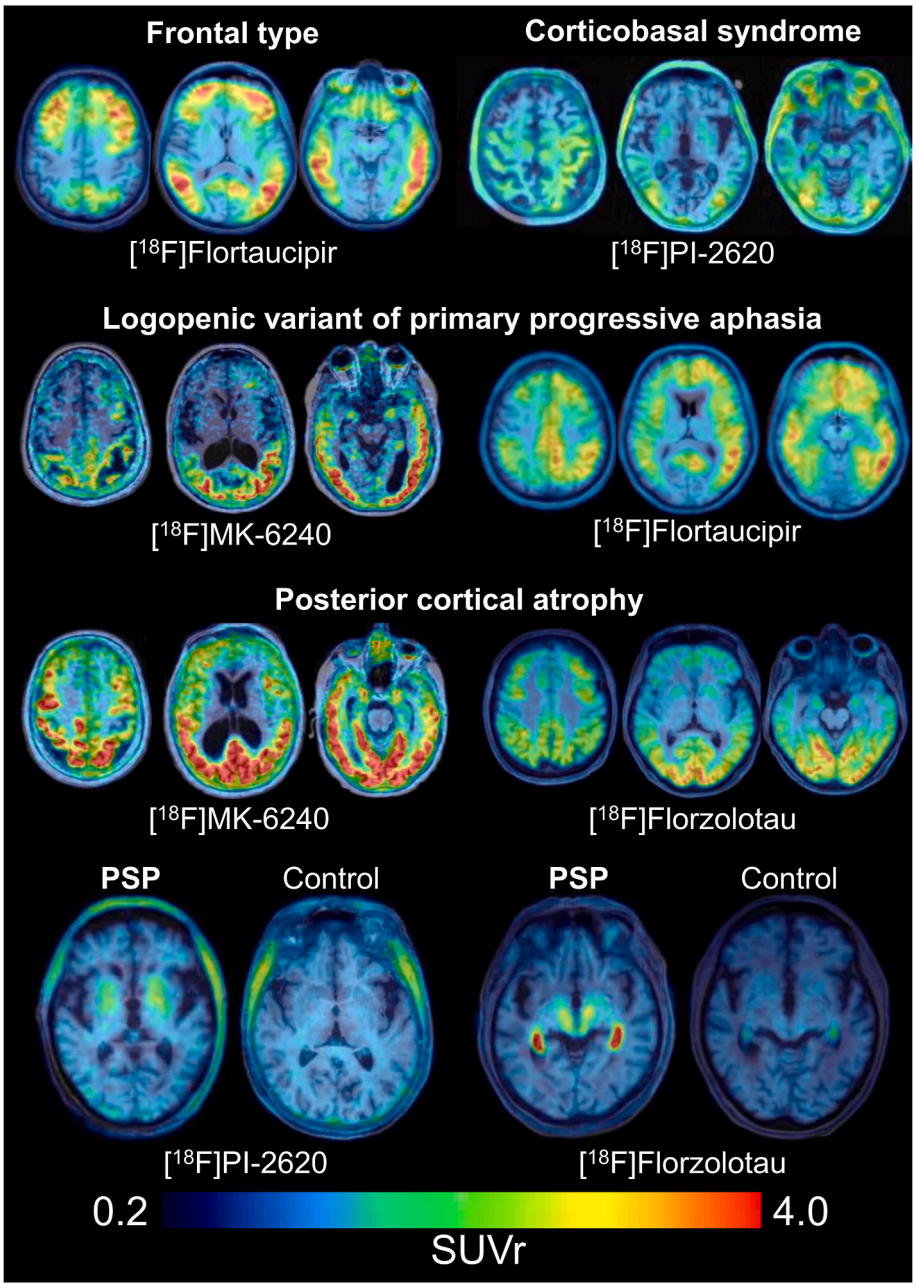

Fig. 3. Examples of tau PET patterns in atypical AD and 4R tauopathies. Three axial slices upon MRI or MRI template show radiotracer distribution in exemplary cases of atypical AD and progressive supranuclear palsy (PSP).

neuropathological data) has not yet been published. There exist pragmatic approaches that evaluate [^{18}F]Florzolotau binding in regions according to the Braak staging scheme based on SUV images or SUVR images (scaled to the cerebellar grey matter) using ordinal rating scales [53,98,99].

[^{18}F]MK-6240: For [^{18}F]MK-6240, three visual read methods have been proposed and clinically evaluated for the assessment of AD [103,104,121], however, currently none are FDA or EMA-approved for application in clinical practice. In research settings, the method by Shuping et al. is most commonly used. The methods by Shuping et al. and Krishnadas et al. are comparable in design and appear applicable in clinical practice. Both methods define four categories (roughly overlapping between the two methods) for the rating of an [^{18}F]MK-6240 image: *negative, MTL-positive, MTL-sparing/minimal MTL uptake* and *typical AD*. There are slight differences in these categories, e.g. while in the Shuping method increased intensity in the entorhinal cortex is considered MTL-positive, this is considered negative in the Krishnadas method. Both methods reach high inter-rater agreement with Cohen's kappa's 0.86 and 0.99 resp. Seibyl et al. propose a visual read algorithm, consisting of a binary read-out, assessments per region and an estimation of spatial extent, for use in clinical trials. All three methods use the inverted grey scale and intensity range is adjusted relative to the cerebellum, to identify areas of radiotracer retention above the activity in the cerebellar reference region (Shuping et al. additionally describe that the intensity in the retina should be set high). In these methods anatomical MRI of CT images were not required. Overall, the visual read methods for the [^{18}F]MK-6240 radiotracer are likely more sensitive to detect AD pathology than the approved visual read method for the assessment of [^{18}F]Flortaucipir scans as increased activity in the MTL region can lead to a positive rating using [^{18}F]MK-6240 visual read methods. The assessment of radiotracer uptake in the MTL region may be more reliable with [^{18}F]MK-6240 than with [^{18}F]Flortaucipir, as

off-target binding in the choroid plexus is minimal for [^{18}F]MK-6240.

[^{18}F]PI-2620: While the performance of a visual read method for the identification of 4R tauopathies using [^{18}F]PI-2620 has been assessed [77,107], efforts for the development of a method specifically aimed at the diagnosis of AD are still ongoing. Bauer et al. demonstrated though that there was high sensitivity (>85%) and specificity (100%) and high inter-rater agreement to distinguish AD from healthy controls with a method rating the scans as *4R tauopathy, AD tauopathy* and *non-tauopathy* in a rainbow-like color scale. Intensity scaling to the cerebellum by using a threshold of 1.0 x mean uptake in the cerebellum may improve the sensitivity (particular for the 40-60 min post injection imaging window). Neither the radiotracer, nor the algorithm have been approved by FDA or EMA for clinical use.

[^{18}F]RO948: Until now only one visual read algorithm for detection of AD related pathology has been published for [^{18}F]RO948 [108]. Compared to [^{18}F]Flortaucipir [122] and [^{18}F]PI-2620 [123], [^{18}F]RO948 shows a higher off-target binding to the skull/meninges, but also a lower off-target binding to the choroid plexus. In the visual read protocol images are assessed using a rainbow color scale with the reference cerebellar grey matter set at the blue to cyan color shift. Attenuation correction CT scans or other structural CT or MRI scans can be used to provide additional anatomical detail and to assess whether suspected off-target binding localizes to bone/meningeal structures, but are not required for the algorithm. Radiotracer retention in the medial temporal lobes/entorhinal cortex, the temporal cortices, and other neocortical regions are assessed. Scans are assigned into one out of four categories: a) *no discernible [^{18}F]RO948 retention or non-AD pattern*; b) [^{18}F]RO948 restricted to the temporal lobes. Unilateral isolated uptake in the medial temporal lobe is considered enough for a positive scan (*early AD*); c) retention of [^{18}F]RO948 in the parietal, occipital or frontal lobes (*late AD*); or d) *inconclusive scan*. Inconclusive scans are scans where the medial temporal lobe signal cannot clearly be attributed to an early AD pattern or where meningeal/skull off-target signal interferes with a potential early uptake. These scans constitute approximately 5-7% of scans and have been considered negative in binary AD/non-AD analyses. The visual read protocol has a high inter-rater reliability with a weighted Cohen's kappa of 0.87 [confidence interval 0.82-0.93]. The visual read algorithm has not been validated against neuropathology in RO948 scans, but validations against quantitative measures of tau and neuropathology in [^{18}F]Flortaucipir scans are underway. The visual read algorithm shows a very high concordance between [^{18}F]RO948 and [^{18}F]Flortaucipir scans ($\kappa = 0.94$ [0.86-1.00]). Neither the radiotracer, nor the algorithm have been approved by FDA or EMA for clinical use.

5.2. Image quantification

Tau PET images are currently quantified using a variety of analytical approaches, and the optimal method remains a topic of ongoing discussion, as suitability often depends on the specific research question or clinical objective [124,125]. Among available metrics, SUVRs are the most widely used due to their practicality and simplicity. Other metrics, such as the DVR derived from dynamic PET scans with kinetic modeling, provide more quantitative estimates of radiotracer binding but require longer acquisition times and more complex analysis pipelines. In practice, a static SUVR measurement acquired during the radiotracer-specific appropriate post injection window yields estimates closely aligned with DVR, making SUVR the preferred choice in most settings.

SUVRs quantify regional radiotracer retention by comparing activity in target regions to a reference region assumed to be largely unaffected by tau pathology as well as influence from off-target binding. The inferior cerebellar cortex is the most commonly used for this purpose, as is the case for [^{18}F]Flortaucipir and [^{18}F]MK-6240 [67,126]. Alternative reference regions, including white matter regions, have been proposed [127,128], but these may be more vulnerable to confounding effects from white matter lesions, spill-over from cortical regions, and age-related structural changes, potentially introducing bias [129]. Despite these considerations, SUVRs demonstrate excellent test–retest reliability, with variability typically below 5%, supporting their robustness as a quantitative metric [23,69,25,89,95,96]. In addition, tau PET has proven to be a sensitive marker of tau accumulation over time in longitudinal studies, with measurable within-subject changes observed over one to two years in both clinical and preclinical populations [71,130,131]. This capacity to detect progression reinforces the utility of tau PET as endpoint in clinical trials, particularly those aiming to evaluate disease-modifying therapies targeting tau pathology.

SUVR quantification is usually performed in anatomically defined cortical regions of interest (ROIs), by averaging SUVR within an ROI or a combination of ROIs (composite ROI). Given its role as the initial site of tau accumulation in AD, the MTL is a critical area for assessment. Another widely used example is the temporal meta-ROI [132], which includes the MTL structures entorhinal cortex, amygdala and parahippocampal gyrus, alongside the lateral inferior and middle temporal and fusiform gyrus, some of these areas are known to accumulate tau in early to intermediate stages of AD. Larger composites, such as larger neocortical or whole-cortex averages, are also used to assess global tau burden [96,133]. Another commonly applied framework is PET-based Braak staging [12,134], in which average SUVRs are computed within ROI sets approximating the anatomical boundaries of Braak stages I–VI. This method attempts to mirror the hierarchical spread of tau pathology observed in postmortem studies. However, it is important to note that this should not be equated with neuropathological Braak staging: current PET-to-autopsy studies indicate that [^{18}F]Flortaucipir primarily detect later-stage pathology, particularly corresponding to Braak stages V–VI, and may lack sensitivity to the earliest phases of disease progression [11,42–44]. In this context, it needs to be repeated, however, that the currently suggested reading methods for Flortaucipir (i.e. instructions to ignore/read as negative isolated ventral & mesial temporal or frontal radiotracer uptake) may systematically shift the sensitivity of the method towards later stages. Second-generation tau PET radiotracers still lack robust post-mortem validations.

In recent years, advanced quantification methods have emerged to complement traditional regional SUVR analyses. While these emerging approaches show promise and may outperform traditional SUVR metrics in specific contexts, their clinical utility remains to be fully established before recommendation of their use can be considered. For example, the novel algorithm TauIQ has demonstrated increased sensitivity for longitudinal analyses and improved early detection of tau deposition [135]. Additional approaches include spatial and network-based models that either capture the propagation of tau along brain networks or identify data-driven patterns of tau accumulation [136,137]. For example, *spatial extent* concurrently assesses tau intensity and tau spatial spread [138,139]. Another approach based on *tau propagation modeling,* uses connectivity-informed frameworks (e.g. diffusion models) to predict how tau accumulates across connected regions over time [140]. Novel *"fill-state"* metrics have also been introduced to quantify the spatial extent of tau PET signal [141]; a fill-state represents the fraction of voxels in the brain that exceed a tau uptake threshold, essentially measuring how tau spreads through expected regions. Further validation is needed across radiotracers and disease stages, as well as in the context of clinical trials, before these methods can be considered for reliable use. For now, static SUVR quantification remains the standard approach in both research and clinical trials due to its simplicity, reproducibility, and wide availability.

Partial-volume effect correction (PVC) is an optional post-processing step used to improve the accuracy of tau PET quantification by accounting for the effects of brain atrophy, spill out, and spill-in from adjacent structures. Tau PET is often applied in aging and AD populations, where significant cortical thinning can lead to underestimation of radiotracer uptake due to partial volume effects. Tau PET also presents radiotracer-specific partial volume challenges. For [^{18}F]Flortaucipir, spill-in of nonspecific signal from the choroid plexus can confound

uptake estimates in adjacent structures like the hippocampus [41,126]. In contrast, second-generation tau radiotracers (e.g., [^{18}F]MK-6240, [^{18}F]PI-2620) are more commonly affected by off-target binding in the meninges and skull, which can introduce spill-in to nearby cortical regions [105,142]. PVC techniques may help mitigate these effects, but their effectiveness depends heavily on the chosen algorithm and the accuracy of anatomical segmentation (which often requires MR imaging) and of the point spread function modelling. Moreover, PVC can increase variability and its added value in longitudinal tau PET studies remains uncertain [143]. As a result, the use of PVC remains inconsistent across studies. SUVR-based quantification—employing carefully selected reference regions and ROI composites—remains the standard approach for assessing tau radiotracer uptake, while there is no evidence that allows recommending the use of PVC in current tau PET practice.

Finally, alongside advances in quantification techniques, novel harmonization methods have been developed to support the comparison of tau PET quantitative metrics across different radiotracers—a critical step toward broader applicability in both clinical and research settings. Approaches such as CenTauR [133,144] and Uniτ [145] aim to standardize SUVR measurements by defining a universal scale for tau burden that can be applied to predefined regions of interest, such as the meta-temporal ROI. Uniτ is additionally designed to harmonize entire 3D tau PET images without the need for pre-established regions. Initial findings indicate that inter-radiotracer harmonization of SUVR values in regions of interest and in entire 3D PET images is feasible [144,145], enabling the pooling and comparison of data across cohorts imaged with different tau PET radiotracers. However, these harmonization methods are still under development and require further validation in independent datasets. In addition, more work is needed to characterize how technical factors—such as scanner model, reconstruction algorithms, and image processing pipelines—may influence the accuracy and reliability of harmonized metrics. Establishing standardized, reproducible harmonization frameworks will be essential for integrating tau PET data across multi-center studies and clinical trials, particularly as the use of second-generation radiotracers continues to expand.

6. Documentation and reporting

6.1. Indications

Patient's name and other identifier (date of birth, name of the referring physician(s), type and date of examination) and patient's history including the reason for requesting the study are mandatory parts of the report.

6.2. Technique

The following items should be noted: name of the imaging radiopharmaceutical used, administered activity of radiopharmaceutical, time between injection of radiopharmaceutical and start of scan, and the imaging technology used (PET, PET/CT, or PET/MRI). When necessary, any issues that may have affected scan quality should be described, e.g. motion artifacts, difficulty with radiopharmaceutical injection (particularly infiltration). Details on equipment specification, quality control, radiation safety, infection control, and patient education concerns are provided in the **Supplement**.

6.3. Findings

- Report on different areas that show increased radiotracer retention. This includes MTL, lateral temporal lobe, parietal/occipital/frontal lobes, motor cortex
- Indicate low, intermediate, or high signal increase
- Consider non-AD tauopathy binding patterns with different predilection sites compared to AD topology (e.g. striatal radiotracer uptake in 4R tauopathies for [^{18}F]Florzolotau and [^{18}F]PI-2620)
- Consider non-specific uptake in regions with hemorrhage, post-ischemia or severe neurodegeneration (e.g. posterior putamen in MSA)
- Indicate if high off-target is present in structures adjacent to the brain
- Describe any anatomical abnormalities detected on the accompanying CT or MRI

6.4. Impression

Interpretation and conclusion

- Positive or negative scan
- Consistent or inconsistent with AD tau pathology beyond the very early stages. Consider reporting of “possible early tauopathy” when elevated signals are restricted to mesio temporal lobes
- Consistent or inconsistent with clinical severity and patterns of neurodegeneration (if available)
- Describe the pattern of AD or non-AD pathology. Reporting on subtypes of regional tau PET spread patterns, such as posterior cortical atrophy, primary progressive aphasia, corticobasal syndrome, or frontal predominant could be considered (examples are provided in Fig. 3). In this regard, consider that clinically overlapping syndromes and similar tau PET pattern topology can relate to distinct molecular tauopathies [78,146,147].

Liability statement

This guideline summarises the views of the EANM Neuroimaging Committee and the SNMMI. It reflects recommendations for which the EANM cannot be held responsible. The recommendations should be considered in the context of good practice in nuclear medicine and do not replace national and international legal or regulatory requirements.

CRediT authorship contribution statement

Matthias Brendel: Writing – review & editing, Writing – original draft, Visualization, Project administration, Conceptualization. **Phillip H. Kuo:** Writing – review & editing, Writing – original draft, Conceptualization. **Joachim Brumberg:** Writing – review & editing, Writing – original draft. **Vincent Doré:** Writing – review & editing, Writing – original draft. **Alexander Drzezga:** Writing – review & editing, Writing – original draft. **Valentina Garibotto:** Writing – review & editing, Writing – original draft. **Antoine Leuzy:** Writing – review & editing, Writing – original draft. **Gregory Mathoux:** Writing – review & editing, Writing – original draft. **Philipp T. Meyer:** Writing – review & editing, Writing – original draft. **Alexis Moscoso:** Writing – review & editing, Writing – original draft. **Rik Ossenkoppele:** Writing – review & editing, Writing – original draft. **Tharick Pascoal:** Writing – review & editing, Writing – original draft. **Ruben Smith:** Writing – review & editing, Writing – original draft. **John Seibyl:** Writing – review & editing, Writing – original draft. **Elsmarieke van de Giessen:** Writing – review & editing, Writing – original draft. **Donatienne Van Weehaeghe:** Writing – review & editing, Writing – original draft. **Marie R. Vermeiren:** Writing – review & editing, Writing – original draft. **Victor L. Villemagne:** Writing – review & editing, Writing – original draft. **Shadi A. Esfahani:** Writing – review & editing, Writing – original draft. **Henryk Barthel:** Writing – review & editing, Writing – original draft, Project administration, Conceptualization. EANM Neuroimaging Committee - Review.

Conflicts of interest

Support Outside this Work

V.L.V. is and has been a consultant or paid speaker at sponsored conference sessions for Eli Lilly, Life Molecular Imaging, ACE Barcelona, IXICO, and Lantheus.

H.B. received research support from Life Molecular Imaging, consulting/speaker honoraria from Hermes Medical Solutions, IBA, Lilly, Eisai, Novartis/AAA and GE, reader honoraria from Life Molecular Imaging, dosing committee honoraria from Pharmtrace, and scientific advisory board honoraria from SOFIE and Positrigo.

M.B. has received speaker honoraria from Roche, GE Healthcare, Iba, Miltenyi, and Life Molecular Imaging; has advised Life Molecular Imaging, MIAC, Cenos, and GE healthcare; and is currently on the advisory or imaging review boards of AC Immune and ZRO Imaging.

M.B. was funded by the Deutsche Forschungsgemeinschaft (DFG) under Germany's Excellence Strategy within the framework of the Munich Cluster for Systems Neurology (EXC 2145 SyNergy – ID 390857198).

R.S. has received consultancy/speaker fees from Eli Lilly, Novo Nordisk, Roche and Triolab.

A.D. received Research support from Siemens Healthineers, Life Molecular Imaging, GE Healthcare, AVID Radiopharmaceuticals, Sofie, Eisai, Novartis/AAA, Ariceum Therapeutics as well as Speaker Honorary/Advisory Boards from Siemens Healthineers, Sanofi, GE Healthcare, Biogen, Novo Nordisk, Invicro, Novartis/AAA, Bayer Vital, Lilly, Peer View Institute for Medical Education, International Atomic Energy Agency, Swiss Rockets. AD owns Stock from Siemens Healthineers, Lantheus Holding, Lilly and a Patent for 18F-JK-PSMA- 7 (Patent No.: EP3765097A1; Date of patent: Jan. 20, 2021).

D.V.W. has received research support and speaker honoraria from General Electric, consulting honoraria from Eli Lilly and reader honoraria from Life Molecular Imaging.

Other activities

A.D. Trials: Participation including PI-roles in industry-sponsored trials. Grants: National and international grants including DFG Grants SFB 1451 C04, DR 445/9-1, Wellcome Leap. Memberships: Societies: DGN, EANM, SNMMI, RSNA, AAIC, etc. Positions: Associate Editor The Journal of Nuclear Medicine, Chair Working Group Neuroscience, DGN, Member Radiation Protection Committee, Member Radiation protection committee, DGN, etc.

V.G. is an Editorial Board member of The EANM Journal but was not involved in any way in the evaluation, revision, or decision process of this article.

SAE is supported by National Cancer Institute (K08CA259626), and has research grants from SOFIE, Telix, Novartis and Lilly, unrelated to this work. SAE is a consultant for Telix.

Acknowledgements

The guidelines have been brought to the attention of the relevant EANM Committees and Councils and the National Societies of Nuclear Medicine in Europe as defined in the EANM statutes. The received comments and suggestions of the EANM members are highly appreciated and have been considered for this guideline.

Images were kindly provided by Amsterdam University Medical Center, LMU Hospital, University Hospital of Cologne, the HEAD study, Medical Center – University of Freiburg and Genentech.

Appendix A. Supplementary data

Supplementary data to this article can be found online at https://doi.org/10.1016/j.eanmj.2026.100214.

Data availability

No data was used for the research described in the article.

References

[1] Braak H, Braak E. Neuropathological stageing of Alzheimer-related changes. Acta Neuropathol 1991;82(4):239–59. PubMed PMID: 1759558.

[2] Jack Jr CR, Bennett DA, Blennow K, Carrillo MC, Dunn B, Haeberlein SB, et al. NIA-AA Research Framework: toward a biological definition of Alzheimer's disease. Alzheimer's Dement 2018 Apr;14(4):535–62. PubMed PMID: 29653606. PMCID: PMC5958625. Epub 2018/04/15. eng.

[3] Jack Jr CR, Bennett DA, Blennow K, Carrillo MC, Feldman HH, Frisoni GB, et al. A/T/N: an unbiased descriptive classification scheme for Alzheimer disease biomarkers. Neurology 2016 Aug 2;87(5):539–47. PubMed PMID: 27371494. PMCID: PMC4970664. Epub 20160701. eng.

[4] Jack JrCR, Andrews JS, Beach TG, Buracchio T, Dunn B, Graf A, et al. Revised criteria for diagnosis and staging of Alzheimer's disease: Alzheimer's Association Workgroup. Alzheimer's Dement 2024;20(8):5143–69.

[5] DeTure MA, Dickson DW. The neuropathological diagnosis of Alzheimer's disease. Mol Neurodegener 2019 Aug 2;14(1):32. PubMed PMID: 31375134. PMCID: PMC6679484. Epub 20190802. eng.

[6] Braak H, Alafuzoff I, Arzberger T, Kretzschmar H, Del Tredici K. Staging of Alzheimer disease-associated neurofibrillary pathology using paraffin sections and immunocytochemistry. Acta Neuropathol 2006 Oct;112(4):389–404. PubMed PMID: 16906426. PMCID: PMC3906709. Epub 20060812. eng.

[7] Goedert M, Spillantini MG, Jakes R, Rutherford D, Crowther RA. Multiple isoforms of human microtubule-associated protein tau: sequences and localization in neurofibrillary tangles of Alzheimer's disease. Neuron 1989 Oct;3(4):519–26. PubMed PMID: 2484340. eng.

[8] Uchihara T. Neurofibrillary changes undergoing morphological and biochemical changes - how does tau with the profile shift of from four repeat to three repeat spread in Alzheimer brain? Neuropathology 2020 Oct;40(5):450–9. PubMed PMID: 32698244. Epub 20200722. eng.

[9] Hara M, Hirokawa K, Kamei S, Uchihara T. Isoform transition from four-repeat to three-repeat tau underlies dendrosomatic and regional progression of neurofibrillary pathology. Acta Neuropathol 2013 Apr;125(4):565–79. PubMed PMID: 23407988. Epub 20130214. eng.

[10] Dujardin S, Hyman BT. Tau prion-like propagation: state of the art and current challenges. Adv Exp Med Biol 2019;1184:305–25. PubMed PMID: 32096046. eng.

[11] Fleisher AS, Pontecorvo MJ, Devous Sr MD, Lu M, Arora AK, Truocchio SP, et al. Positron emission tomography imaging with [18F]flortaucipir and postmortem assessment of alzheimer disease neuropathologic changes. JAMA Neurol 2020 Apr 27. PubMed PMID: 32338734. PMCID: PMC7186920. Epub 2020/04/28.

[12] Therriault J, Pascoal TA, Lussier FZ, Tissot C, Chamoun M, Bezgin G, et al. Biomarker modeling of Alzheimer's disease using PET-based Braak staging. Nat Aging 2022 Jun;2(6):526–35. PubMed PMID: 37118445. PMCID: PMC10154209. Epub 20220425. eng.

[13] Ossenkoppele R, Schonhaut DR, Schöll M, Lockhart SN, Ayakta N, Baker SL, et al. Tau PET patterns mirror clinical and neuroanatomical variability in Alzheimer's disease. Brain 2016 May;139(Pt 5):1551–67. PubMed PMID: 26962052. PMCID: PMC5006248. Epub 2016/03/11. eng.

[14] Vogel JW, Young AL, Oxtoby NP, Smith R, Ossenkoppele R, Strandberg OT, et al. Four distinct trajectories of tau deposition identified in Alzheimer's disease. Nat Med 2021 May;27(5):871–81. PubMed PMID: 33927414. PMCID: PMC8686688. Epub 2021/05/01.

[15] Moscoso A, Heeman F, Raghavan S, Costoya-Sánchez A, van Essen M, Mainta I, et al. Frequency and clinical outcomes associated with Tau Positron Emission tomography positivity. JAMA 2025 Jun 16. PubMed PMID: 40522652. Epub 2025/06/16. eng.

[16] Ossenkoppele R, Coomans EM, Apostolova LG, Baker SL, Barthel H, Beach TG, et al. Tau PET positivity in individuals with and without cognitive impairment varies with age, amyloid-β status, APOE genotype and sex. Nat Neurosci 2025. 2025/07/16.

[17] Rabinovici GD, Knopman DS, Arbizu J, Benzinger TLS, Donohoe KJ, Hansson O, et al. Updated appropriate use criteria for amyloid and tau PET: a report from the Alzheimer's association and society for nuclear medicine and molecular imaging workgroup. J Nucl Med 2025;124:268756. jnumed.

[18] Rabinovici GD, Knopman DS, Arbizu J, Benzinger TLS, Donohoe KJ, Hansson O, et al. Updated appropriate use criteria for amyloid and tau PET: a report from the Alzheimer's association and society for nuclear medicine and molecular imaging workgroup. Alzheimer's Dement 2025;21(1):e14338.

[19] Rabinovici GD, Gatsonis C, Apgar C, Chaudhary K, Gareen I, Hanna L, et al. Association of amyloid positron emission tomography with subsequent change in clinical management among medicare beneficiaries with mild cognitive impairment or dementia. JAMA 2019 Apr 2;321(13):1286–94. PubMed PMID: 30938796. PMCID: PMC6450276. eng.

[20] Povala G, Bauer-Negrini G, Bellaver B, Lussier FZ, Amaral L, Ferreira PCL, et al. Universal tau PET scale (Uniτ) – the HEAD study. Alzheimer's & Dementia 2024; 20(S9):e094383.

[21] Jie C, Treyer V, Schibli R, Mu L. Tauvid™: the first FDA-approved PET tracer for imaging Tau pathology in Alzheimer's Disease. Pharmaceuticals 2021 Jan 30;14 (2). PubMed PMID: 33573211. PMCID: PMC7911942. Epub 20210130. eng.

[22] Lin K-J, Huang S-Y, Huang K-L, Huang C-C, Hsiao I-T. Human biodistribution and radiation dosimetry for the tau tracer [18F]Florzolotau in healthy subjects. EJNMMI Radiopharmacy and Chemistry 2024 2024/04/02;9(1):27.

[23] Sanabria Bohórquez S, Marik J, Ogasawara A, Tinianow JN, Gill HS, Barret O, et al. [(18)F]GTP1 (Genentech Tau Probe 1), a radioligand for detecting neurofibrillary tangle tau pathology in Alzheimer's disease. Eur J Nucl Med Mol Imaging 2019 Sep;46(10):2077–89. PubMed PMID: 31254035. Epub 2019/06/30. eng.

[24] Ohnishi A, Akamatsu G, Ikari Y, Nishida H, Shimizu K, Matsumoto K, et al. Dosimetry and efficacy of a tau PET tracer [(18)F]MK-6240 in Japanese healthy

elderly and patients with Alzheimer's disease. Ann Nucl Med 2023 Feb;37(2):108–20. PubMed PMID: 36411357. PMCID: PMC9902412. Epub 20221121. eng.
[25] Bullich S, Barret O, Constantinescu C, Sandiego C, Mueller A, Berndt M, et al. Evaluation of dosimetry, quantitative methods, and test-retest variability of (18)F-PI-2620 PET for the assessment of tau deposits in the human brain. J Nucl Med 2020 Jun;61(6):920–7. PubMed PMID: 31712324. PMCID: PMC7262221. Epub 20191111. eng.
[26] Wong DF, Comley RA, Kuwabara H, Rosenberg PB, Resnick SM, Ostrowitzki S, et al. Characterization of 3 novel tau radiopharmaceuticals, (11)C-RO-963, (11)C-RO-643, and (18)F-RO-948, in healthy controls and in alzheimer subjects. J Nucl Med 2018 Dec;59(12):1869–76. PubMed PMID: 29728519. PMCID: PMC6278896. Epub 2018/05/08. eng.
[27] Boccalini C, Peretti DE, Mathoux G, Iaccarino L, Ribaldi F, Scheffler M, et al. Early-phase (18)F-Flortaucipir tau-PET as a proxy of brain metabolism in Alzheimer's disease: a comparison with (18)F-FDG-PET and early-phase amyloid-PET. Eur J Nucl Med Mol Imaging 2025 May;52(6):1958–69. PubMed PMID: 39849149. PMCID: PMC12014785. Epub 20250124. eng.
[28] Beyer L, Nitschmann A, Barthel H, van Eimeren T, Unterrainer M, Sauerbeck J, et al. Early-phase [(18)F]PI-2620 tau-PET imaging as a surrogate marker of neuronal injury. Eur J Nucl Med Mol Imaging 2020 Nov;47(12):2911–22. PubMed PMID: 32318783. PMCID: PMC7567714. Epub 20200421. eng.
[29] Guehl NJ, Dhaynaut M, Hanseeuw BJ, Moon SH, Lois C, Thibault E, et al. Measurement of cerebral perfusion indices from the early phase of [(18)F]MK6240 dynamic tau PET imaging. J Nucl Med 2023 Jun;64(6):968–75. PubMed PMID: 36997330. PMCID: PMC10241011. Epub 20230330. eng.
[30] Hammes J, Leuwer I, Bischof GN, Drzezga A, van Eimeren T. Multimodal correlation of dynamic [(18)F]-AV-1451 perfusion PET and neuronal hypometabolism in [(18)F]-FDG PET. Eur J Nucl Med Mol Imaging 2017 Dec;44(13):2249–56. PubMed PMID: 29026951. Epub 20171012. eng.
[31] EMA label for [18F]flortaucipir [Available from: https://www.ema.europa.eu/en/medicines/human/EPAR/tauvid].
[32] FDA label for [18F]flortaucipir [Available from: https://www.accessdata.fda.gov/drugsatfda_docs/label/2020/212123s000lbl.pdf].
[33] Leuzy A, Chiotis K, Lemoine L, Gillberg PG, Almkvist O, Rodriguez-Vieitez E, et al. Tau PET imaging in neurodegenerative tauopathies-still a challenge. Mol Psychiatr 2019 Aug;24(8):1112–34. PubMed PMID: 30635637. PMCID: PMC6756230. Epub 2019/01/13.
[34] Vermeiren C, Motte P, Viot D, Mairet-Coello G, Courade JP, Citron M, et al. The tau positron-emission tomography tracer AV-1451 binds with similar affinities to tau fibrils and monoamine oxidases. Mov Disord 2018 Feb;33(2):273–81. PubMed PMID: 29278274. Epub 2017/12/27. eng.
[35] Hansen AK, Brooks DJ, Borghammer P. MAO-B inhibitors do not block in vivo Flortaucipir([(18)F]-AV-1451) binding. Mol Imaging Biol 2018 Jun;20(3):356–60. PubMed PMID: 29127552.
[36] Smith R, Schöll M, Londos E, Ohlsson T, Hansson O. (18)F-AV-1451 in Parkinson's Disease with and without dementia and in Dementia with Lewy Bodies. Sci Rep 2018 Mar 16;8(1):4717. PubMed PMID: 29549278. PMCID: PMC5856779 (for the institution) from Roche, GE Healthcare, Biogen, AVID Radiopharmaceuticals, Fujirebio, and Euroimmun. In the past 2 years, he has received consultancy/speaker fees (paid to the institution) from Lilly, Roche, and Fujirebio. Epub 2018/03/20. eng.
[37] Marquie M, Normandin MD, Vanderburg CR, Costantino IM, Bien EA, Rycyna LG, et al. Validating novel tau positron emission tomography tracer [F-18]-AV-1451 (T807) on postmortem brain tissue. Ann Neurol 2015 Nov;78(5):787–800. PubMed PMID: 26344059.
[38] Lowe VJ, Curran G, Fang P, Liesinger AM, Josephs KA, Parisi JE, et al. An autoradiographic evaluation of AV-1451 Tau PET in dementia. Acta Neuropathol Commun 2016 Jun 13;4(1):58. PubMed PMID: 27296779. PMCID: PMC4906968. Epub 20160613. eng.
[39] Marquie M, Verwer EE, Meltzer AC, Kim SJW, Aguero C, Gonzalez J, et al. Lessons learned about [F-18]-AV-1451 off-target binding from an autopsy-confirmed Parkinson's case. Acta Neuropathol Commun 2017 Oct 19;5(1):75. PubMed PMID: 29047416. PMCID: PMC5648451. Epub 20171019.
[40] Choi JY, Cho H, Ahn SJ, Lee JH, Ryu YH, Lee MS, et al. Off-Target (18)F-AV-1451 binding in the basal ganglia correlates with age-related iron accumulation. J Nucl Med 2018 Jan;59(1):117–20. PubMed PMID: 28775201. Epub 2017/08/05.
[41] Lopez-Gonzalez FJ, Costoya-Sanchez A, Paredes-Pacheco J, Moscoso A, Silva-Rodriguez J, Aguiar P, et al. Impact of spill-in counts from off-target regions on [(18)F]Flortaucipir PET quantification. Neuroimage 2022 Oct 1;259:119396. PubMed PMID: 35753593. Epub 2022/06/27.
[42] Moscoso A, Wren MC, Lashley T, Arstad E, Murray ME, Fox NC, et al. Imaging tau pathology in Alzheimer's disease with positron emission tomography: lessons learned from imaging-neuropathology validation studies. Mol Neurodegener 2022 Jun 3;17(1):39. PubMed PMID: 35659709. PMCID: PMC9166480. Epub 2022/06/07.
[43] Lowe VJ, Lundt ES, Albertson SM, Min HK, Fang P, Przybelski SA, et al. Tau-positron emission tomography correlates with neuropathology findings. Alzheimer's Dement 2020 Mar;16(3):561–71. PubMed PMID: 31784374. PMCID: PMC7067654. Epub 2019/12/01.
[44] Soleimani-Meigooni DN, Iaccarino L, La Joie R, Baker S, Bourakova V, Boxer AL, et al. 18F-flortaucipir PET to autopsy comparisons in Alzheimer's disease and other neurodegenerative diseases. Brain 2020 Dec 5;143(11):3477–94. PubMed PMID: 33141172. PMCID: PMC7719031. Epub 2020/11/04. eng.
[45] Freiburghaus T, Pawlik D, Oliveira Hauer K, Ossenkoppele R, Strandberg O, Leuzy A, et al. Association of in vivo retention of [18f] flortaucipir pet with tau neuropathology in corresponding brain regions. Acta Neuropathol 2024 2024/09/19;148(1):44.
[46] Tunali I, Wang J, Arora AK, Kim MJ, Shcherbinin S, Pontecorvo M, et al. Development and validation of a (18)F-Flortaucipir PET visual stratification method. J Nucl Med 2025 Mar 13;66(4):612–9. PubMed PMID: 40081955. PMCID: PMC11960607. Epub 2025/03/14. eng.
[47] Sims JR, Zimmer JA, Evans CD, Lu M, Ardayfio P, Sparks J, et al. Donanemab in early symptomatic alzheimer disease: the TRAILBLAZER-ALZ 2 randomized clinical trial. JAMA 2023 Aug 8;330(6):512–27. PubMed PMID: 37459141. PMCID: PMC10352931.
[48] Mintun MA, Lo AC, Duggan Evans C, Wessels AM, Ardayfio PA, Andersen SW, et al. Donanemab in early Alzheimer's Disease. N Engl J Med 2021 May 6;384(18):1691–704. PubMed PMID: 33720637. Epub 20210313.
[49] Sperling RA, Rentz DM, Johnson KA, Karlawish J, Donohue M, Salmon DP, et al. The A4 study: stopping AD before symptoms begin? Sci Transl Med 2014 Mar 19;6(228). 228fs13. PubMed PMID: 24648338. PMCID: PMC4049292. Epub 2014/03/22.
[50] Fleisher AS, Munsie LM, Perahia DGS, Andersen SW, Higgins IA, Hauck PM, et al. Assessment of efficacy and safety of Zagotenemab: results from PERISCOPE-ALZ, a phase 2 Study in early symptomatic alzheimer disease. Neurology 2024 Mar 12;102(5):e208061. PubMed PMID: 38386949. PMCID: PMC11067698. Epub 20240222.
[51] PROSPECT-ALZ: results of the phase 2 study of ceperognastat, an orally available O-linked N-acetyl glucosaminidase inhibitor for the treatment of early symptomatic Alzheimer's disease [Available from: https://assets.ctfassets.net/mpejy6umgthp/jLMZSYBfH43BzC2NJDejW/cbaa5093c20034b60118fb565733c804/DV-022295_OC10_MTAE_Fleisher_V2-2024_1029-MDD.pdf.
[52] Tagai K, Ono M, Kubota M, Kitamura S, Takahata K, Seki C, et al. High-contrast in vivo imaging of tau pathologies in alzheimer's and non-alzheimer's disease tauopathies. Neuron 2021 Jan 6;109(1):42–58.e8. PubMed PMID: 33125873. Epub 2020/10/31. eng.
[53] Brumberg J, Schröter N, Blazhenets G, Omrane MA, Volz C, Weiller C, et al. [(18)F]Florzolotau PET for the differential diagnosis of parkinsonism in patients with suspected 4-Repeat tauopathies. J Nucl Med 2025 Apr 17. PubMed PMID: 40246540. Epub 2025/04/18. eng.
[54] Li L, Liu FT, Li M, Lu JY, Sun YM, Liang X, et al. Clinical utility of (18) F-APN-1607 tau PET imaging in patients with progressive supranuclear palsy. Mov Disord 2021 Oct;36(10):2314–23. PubMed PMID: 34089275. Epub 2021/06/06. eng.
[55] Liu FT, Lu JY, Li XY, Jiao FY, Chen MJ, Yao RX, et al. (18) F-Florzolotau positron emission tomography imaging of Tau pathology in the living brains of patients with corticobasal syndrome. Mov Disord 2023 Apr;38(4):579–88. PubMed PMID: 36750757. Epub 2023/02/09. eng.
[56] Blazhenets G, Brumberg J, Endo H, Hsu J-L, Frings L, Schroeter N, et al. Voxel-wise Florzolotau (APN-1607) tau PET covariance patterns in alzheimer's disease and progressive supranuclear Palsy. Alzheimer's & Dementia 2024;20(S9):e094066.
[57] Endo H, Araki N, Takeda T, Takado Y, Tagai K, Matsuoka K, et al. Correlation of 18F-PM-PBB3 (18F-florzolotau) tau PET imaging with postmortem neuropathological findings in A case with progressive supranuclear palsy (P9-11.015). Neurology 2023;100(17_supplement_2):1334.
[58] Suzuki H, Kubota M, Kurose S, Tagai K, Endo H, Onaya M, et al. Neuropathological correlations of 18F-florzolotau PET in a case with Pick's disease. EJNMMI Res 2025 2025/07/31;15(1):96.
[59] Koga S, Metrick 2nd MA, Golbe LI, Santambrogio A, Kim M, Soto-Beasley AI, et al. Case report of a patient with unclassified tauopathy with molecular and neuropathological features of both progressive supranuclear palsy and corticobasal degeneration. Acta Neuropathol Commun 2023 Jun 1;11(1):88. PubMed PMID: 37264457. PMCID: PMC10236843. Epub 20230601. eng.
[60] Teng E, Manser PT, Sanabria Bohorquez S, Wildsmith KR, Pickthorn K, Baker SL, et al. Baseline [(18)F]GTP1 tau PET imaging is associated with subsequent cognitive decline in Alzheimer's disease. Alzheimers Res Ther 2021 Dec 1;13(1):196. PubMed PMID: 34852837. PMCID: PMC8638526. Epub 20211201.
[61] Teng E, Ward M, Manser PT, Sanabria-Bohorquez S, Ray RD, Wildsmith KR, et al. Cross-sectional associations between [(18)F]GTP1 tau PET and cognition in Alzheimer's disease. Neurobiol Aging 2019 Sep;81:138–45. PubMed PMID: 31280117. Epub 2019/07/08. eng.
[62] Sanabria Bohorquez SM, Baker S, Manser PT, Tonietto M, Galli C, Wildsmith KR, et al. Evaluation of partial volume correction and analysis of longitudinal [(18)F]GTP1 tau PET imaging in Alzheimer's disease using linear mixed-effects models. Front Neuroimaging 2024;3:1355402. PubMed PMID: 38606196. PMCID: PMC11008283. Epub 20240328.
[63] Olafson E, Tonietto M, Klein G, Teng E, Stephens AW, Russell DS, et al. In vivo head-to-head comparison of [(18)F]GTP1 with [(18)F]MK-6240 and [(18)F]PI-2620 in alzheimer disease. J Nucl Med 2025 Feb 3;66(2):277–85. PubMed PMID: 39746756. PMCID: PMC11800736. Epub 20250203.
[64] Kunach P, Vaquer-Alicea J, Smith MS, Monistrol J, Hopewell R, Moquin L, et al. Cryo-EM structure of Alzheimer's disease tau filaments with PET ligand MK-6240. Nat Commun 2024 Oct 1;15(1):8497. PubMed PMID: 39353896. PMCID: PMC11445244. Epub 2024/10/02. eng.
[65] Betthauser TJ, Cody KA, Zammit MD, Murali D, Converse AK, Barnhart TE, et al. In vivo characterization and quantification of Neurofibrillary Tau PET Radioligand (18)F-MK-6240 in humans from alzheimer disease dementia to young controls. J Nucl Med 2019 Jan;60(1):93–9. PubMed PMID: 29777006. PMCID: PMC6354223. Epub 2018/05/20. eng.

[66] Lohith TG, Bennacef I, Vandenberghe R, Vandenbulcke M, Salinas CA, Declercq R, et al. Brain imaging of alzheimer dementia patients and elderly controls with (18)F-MK-6240, a PET tracer targeting neurofibrillary tangles. J Nucl Med 2019 Jan;60(1):107–14. PubMed PMID: 29880509. Epub 2018/06/09. eng.
[67] Pascoal TA, Shin M, Kang MS, Chamoun M, Chartrand D, Mathotaarachchi S, et al. In vivo quantification of neurofibrillary tangles with [(18)F]MK-6240. Alzheimers Res Ther 2018 Jul 31;10(1):74. PubMed PMID: 30064520. PMCID: PMC6069775. Epub 2018/08/02. eng.
[68] Gogola A, Minhas DS, Villemagne VL, Cohen AD, Mountz JM, Pascoal TA, et al. Direct comparison of the tau PET tracers (18)F-Flortaucipir and (18)F-MK-6240 in human subjects. J Nucl Med 2022 Jan;63(1):108–16. PubMed PMID: 33863821. PMCID: PMC8717175. Epub 2021/04/18. eng.
[69] Salinas C, Lohith TG, Purohit A, Struyk A, Sur C, Bennacef I, et al. Test-retest characteristic of [(18)F]MK-6240 quantitative outcomes in cognitively normal adults and subjects with Alzheimer's disease. J Cereb Blood Flow Metab 2020 Nov;40(11):2179–87. PubMed PMID: 31711342. PMCID: PMC7585918. Epub 2019/11/13. eng.
[70] Vanderlinden G, Mertens N, Michiels L, Lemmens R, Koole M, Vandenbulcke M, et al. Long-term test-retest of cerebral [(18)F]MK-6240 binding and longitudinal evaluation of extracerebral tracer uptake in healthy controls and amnestic MCI patients. Eur J Nucl Med Mol Imaging 2022 Nov;49(13):4580–8. PubMed PMID: 35852556. Epub 2022/07/20. eng.
[71] Pascoal TA, Benedet AL, Tudorascu DL, Therriault J, Mathotaarachchi S, Savard M, et al. Longitudinal 18F-MK-6240 tau tangles accumulation follows Braak stages. Brain 2021 Dec 16;144(11):3517–28. PubMed PMID: 34515754. PMCID: PMC8677534. Epub 2021/09/14. eng.
[72] Mueller A, Bullich S, Barret O, Madonia J, Berndt M, Papin C, et al. Tau PET imaging with (18)F-PI-2620 in patients with alzheimer disease and healthy controls: a first-in-humans Study. J Nucl Med 2020 Jun;61(6):911–9. PubMed PMID: 31712323. PMCID: PMC7262222. Epub 2019/11/13. eng.
[73] Chotipanich C, Nivorn M, Kunawudhi A, Promteangtrong C, Boonkawin N, Jantarato A. Evaluation of imaging windows for tau PET imaging using (18)F-PI2620 in cognitively normal individuals, mild cognitive impairment, and Alzheimer's Disease patients. Mol Imaging 2020 Jan-Dec;19:1536012120947582. PubMed PMID: 32862780. PMCID: PMC7466905. eng.
[74] Song M, Scheifele M, Barthel H, van Eimeren T, Beyer L, Marek K, et al. Feasibility of short imaging protocols for [(18)F]PI-2620 tau-PET in progressive supranuclear palsy. Eur J Nucl Med Mol Imaging 2021 Nov;48(12):3872–85. PubMed PMID: 34021393. PMCID: PMC8484138. Epub 20210522. eng.
[75] Mormino EC, Toueg TN, Azevedo C, Castillo JB, Guo W, Nadiadwala A, et al. Tau PET imaging with (18)F-PI-2620 in aging and neurodegenerative diseases. Eur J Nucl Med Mol Imaging 2021 Jul;48(7):2233–44. PubMed PMID: 32572562. PMCID: PMC7755737. Epub 2020/06/24. eng.
[76] Blazhenets G, Soleimani-Meigooni DN, Thomas W, Mundada N, Brendel M, Vento S, et al. [(18)F]PI-2620 binding patterns in patients with suspected alzheimer disease and frontotemporal lobar degeneration. J Nucl Med 2023 Dec 1;64(12):1980–9. PubMed PMID: 37918868. PMCID: PMC10690126. Epub 20231201. eng.
[77] Brendel M, Barthel H, van Eimeren T, Marek K, Beyer L, Song M, et al. Assessment of 18F-PI-2620 as a biomarker in progressive supranuclear palsy. JAMA Neurol 2020 Nov 1;77(11):1408–19. PubMed PMID: 33165511. PMCID: PMC7341407.
[78] Palleis C, Brendel M, Finze A, Weidinger E, Botzel K, Danek A, et al. Cortical [(18)F]PI-2620 binding Differentiates Corticobasal Syndrome subtypes. Mov Disord 2021 Sep;36(9):2104–15. PubMed PMID: 33951244. Epub 2021/05/06.
[79] Oh M, Oh SJ, Lee SJ, Oh JS, Roh JH, Chung SJ, et al. Clinical evaluation of 18F-PI-2620 as a potent PET radiotracer imaging tau protein in alzheimer disease and other neurodegenerative diseases compared with 18F-THK-5351. Clin Nucl Med 2020 Nov;45(11):841–7. PubMed PMID: 32910050. Epub 2020/09/11. eng.
[80] Aguero C, Dhaynaut M, Amaral AC, Moon SH, Neelamegam R, Scapellato M, et al. Head-to-head comparison of [18F]-Flortaucipir, [18F]-MK-6240 and [18F]-PI-2620 postmortem binding across the spectrum of neurodegenerative diseases. Acta Neuropathol 2024 2024/01/27;147(1):25.
[81] Kling A, Kusche-Palenga J, Palleis C, Jäck A, Bernhardt AM, Frontzkowski L, et al. Exploring the origins of frequent tau-PET signal in vermal and adjacent regions. Eur J Nucl Med Mol Imaging 2025 Mar 18. PubMed PMID: 40100387. Epub 20250318. eng.
[82] Rullmann M, Brendel M, Schroeter ML, Saur D, Levin J, Perneczky RG, et al. Multicenter (18)F-PI-2620 PET for in vivo braak staging of tau pathology in Alzheimer's Disease. Biomolecules 2022 Mar 16;12(3). PubMed PMID: 35327650. PMCID: PMC8946049. Epub 2022/03/26. eng.
[83] Bullich S, Mueller A, De Santi S, Koglin N, Krause S, Kaplow J, et al. Evaluation of tau deposition using (18)F-PI-2620 PET in MCI and early AD subjects-a MissionAD tau sub-study. Alzheimers Res Ther 2022 Jul 27;14(1):105. PubMed PMID: 35897078. PMCID: PMC9327167. Epub 2022/07/28. eng.
[84] Oh M, Oh SJ, Lee SJ, Oh JS, Seo SY, Ryu S, et al. One-Year longitudinal changes in tau accumulation on [(18)F]PI-2620 PET in the alzheimer spectrum. J Nucl Med 2024 Mar 1;65(3):453–61. PubMed PMID: 38302152. Epub 2024/02/02. eng.
[85] Slemann L, Gnörich J, Hummel S, Bartos LM, Klaus C, Kling A, et al. Neuronal and oligodendroglial, but not astroglial, tau translates to in vivo tau PET signals in individuals with primary tauopathies. Acta Neuropathol 2024 Nov 24;148(1):70. PubMed PMID: 39580770. PMCID: PMC11586312. Epub 20241124. eng.
[86] Smith R, Scholl M, Leuzy A, Jogi J, Ohlsson T, Strandberg O, et al. Head-to-head comparison of tau positron emission tomography tracers [(18)F]flortaucipir and [(18)F]RO948. Eur J Nucl Med Mol Imaging 2020 Feb;47(2):342–54. PubMed PMID: 31612245. PMCID: PMC6974501.
[87] Leuzy A, Smith R, Ossenkoppele R, Santillo A, Borroni E, Klein G, et al. Diagnostic performance of RO948 F 18 Tau positron emission tomography in the differentiation of alzheimer disease from other neurodegenerative disorders. JAMA Neurol 2020 Aug 1;77(8):955–65. PubMed PMID: 32391858. PMCID: PMC7215644.
[88] Rodriguez-Gomez O, Sanabria A, Perez-Cordon A, Sanchez-Ruiz D, Abdelnour C, Valero S, et al. FACEHBI: a prospective study of risk factors, biomarkers and cognition in a cohort of individuals with subjective cognitive decline. Study rationale and research protocols. J Prev Alzheimers Dis 2017;4(2):100–8. PubMed PMID: 29186280.
[89] Kuwabara H, Comley RA, Borroni E, Honer M, Kitmiller K, Roberts J, et al. Evaluation of (18)F-RO-948 PET for quantitative assessment of tau accumulation in the human brain. J Nucl Med 2018 Dec;59(12):1877–84. PubMed PMID: 30097505. PMCID: PMC6278898. Epub 2018/08/12.
[90] Leuzy A, Binette AP, Vogel JW, Klein G, Borroni E, Tonietto M, et al. Comparison of group-level and individualized brain regions for measuring change in Longitudinal Tau positron emission tomography in alzheimer disease. JAMA Neurol 2023 Jun 1;80(6):614–23. PubMed PMID: 37155176. PMCID: PMC10167602 from Enigma Biomedical USA outside the submitted work. Drs Klein, Borroni, and Tonietto reported being full-time employees of F. Hoffmann-La Roche during the conduct of the study. Dr Palmqvist reported serving on scientific advisory boards and/or given lectures in symposia sponsored by BioArctic, Biogen, Cytox, Eli Lilly, Geras Solutions, and Roche. Drs Pontecorvo and Iaccarino reported being full-time employees and shareholders of Eli Lilly and Company. Dr Hansson reported receiving nonfinancial support (precursor of RO948 and AVID PET images) from AVID/Eli Lilly during the conduct of the study and consultant/speaker fees from AC Immune, Amylyx, Alzpath, ADx, AVID Radiopharmaceuticals, Biogen, Cerveau, Eli Lilly, Eisai, Fujirebio, Genentech, Novartis, BioArctic, GE Healthcare, Pfizer, Roche, and Siemens outside the submitted work. No other disclosures were reported. Epub 2023/05/08.
[91] Smith R, Strandberg O, Leuzy A, Betthauser TJ, Johnson SC, Pereira JB, et al. Sex differences in off-target binding using tau positron emission tomography. Neuroimage Clin 2021;31:102708. PubMed PMID: 34091353. PMCID: PMC8182304. Epub 2021/06/07. eng.
[92] Honer M, Gobbi L, Knust H, Kuwabara H, Muri D, Koerner M, et al. Preclinical evaluation of (18)F-RO6958948, (11)C-RO6931643, and (11)C-RO6924963 as novel PET radiotracers for imaging tau aggregates in alzheimer disease. J Nucl Med 2018 Apr;59(4):675–81. PubMed PMID: 28970331. PMCID: PMC5932750. Epub 2017/10/04. eng.
[93] Leuzy A, Smith R, Cullen NC, Strandberg O, Vogel JW, Binette AP, et al. Biomarker-based prediction of Longitudinal Tau Positron Emission tomography in alzheimer disease. JAMA Neurol 2022 Feb 1;79(2):149–58. PubMed PMID: 34928318. PMCID: PMC8689441 boards and/or given lectures in symposia sponsored by F. Hoffmann-La Roche, Biogen, and Geras Solutions. Dr Klein reported being a shareholder of F. Hoffmann-La Roche as an employee outside the submitted work. Dr Hansson reported nonfinancial support from F. Hoffmann-La Roche and GE Healthcare during the conduct of the study; and grants from Swedish Research Council during the conduct of the study; personal fees from Biogen, Roche, Cerveau, and Siemens outside the submitted work; research support (for their institution) from AVID Radiopharmaceuticals, Biogen, Eli Lilly, Eisai, GE Healthcare, Pfizer, and Roche; and has received consultancy/speaker fees from Roche, Genentech, Siemens, Biogen, Alzpath, and Cerveau. No other disclosures were reported. Epub 2021/12/21. eng.
[94] Baker SL, Harrison TM, Maass A, La Joie R, Jagust WJ. Effect of off-target binding on (18)F-Flortaucipir variability in healthy controls across the life span. J Nucl Med 2019 Oct;60(10):1444–51. PubMed PMID: 30877180. PMCID: PMC6785795. Epub 2019/03/17.
[95] Timmers T, Ossenkoppele R, Visser D, Tuncel H, Wolters EE, Verfaillie SC, et al. Test-retest repeatability of [(18)F]Flortaucipir PET in Alzheimer's disease and cognitively normal individuals. J Cereb Blood Flow Metab 2020 Dec;40(12):2464–74. PubMed PMID: 31575335. PMCID: PMC7705644. Epub 20191001.
[96] Devous MD Sr, Joshi AD, Navitsky M, Southekal S, Pontecorvo MJ, Shen H, et al. Test-retest reproducibility for the tau PET imaging agent Flortaucipir F 18. J Nucl Med 2018 Jun;59(6):937–43. PubMed PMID: 29284675. Epub 20171228.
[97] Johnson KA, Schultz A, Betensky RA, Becker JA, Sepulcre J, Rentz D, et al. Tau positron emission tomographic imaging in aging and early Alzheimer disease. Ann Neurol 2016 Jan;79(1):110–9. PubMed PMID: 26505746. PMCID: PMC4738026.
[98] Lin HC, Lin KJ, Huang KL, Chen SH, Ho TY, Huang CC, et al. Visual reading for [(18)F]Florzolotau ([(18)F]APN-1607) tau PET imaging in clinical assessment of Alzheimer's disease. Front Neurosci 2023;17:1148054. PubMed PMID: 37250400. PMCID: PMC10213356. Epub 2023/05/30. eng.
[99] Shimohama S, Tezuka T, Takahata K, Bun S, Tabuchi H, Seki M, et al. Impact of amyloid and tau PET on changes in diagnosis and patient management. Neurology 2023 Jan 17;100(3):e264–74. PubMed PMID: 36175151. Epub 2022/09/30. eng.
[100] Liu FT, Li XY, Lu JY, Wu P, Li L, Liang XN, et al. (18) F-Florzolotau tau positron emission tomography imaging in patients with multiple system atrophy-parkinsonian subtype. Mov Disord 2022 Sep;37(9):1915–23. PubMed PMID: 35861378. Epub 2022/07/22. eng.
[101] Lu J, Ju Z, Wang M, Sun X, Jia C, Li L, et al. Feasibility of (18)F-florzolotau quantification in patients with Alzheimer's disease based on an MRI-free tau PET template. Eur Radiol 2023 Jul;33(7):4567–79. PubMed PMID: 37099173. Epub 2023/04/26. eng.
[102] Sanabria Bohórquez SM, Baker S, Manser PT, Tonietto M, Galli C, Wildsmith KR, et al. Evaluation of partial volume correction and analysis of longitudinal [(18)F]

GTP1 tau PET imaging in Alzheimer's disease using linear mixed-effects models. Front Neuroimaging 2024;3:1355402. PubMed PMID: 38606196. PMCID: PMC11008283. Epub 20240328. eng.
[103] Shuping JL, Matthews DC, Adamczuk K, Scott D, Rowe CC, Kreisl WC, et al. Development, initial validation, and application of a visual read method for [(18)F]MK-6240 tau PET. Alzheimer's Dement 2023 Jan-Mar;9(1):e12372. PubMed PMID: 36873926. PMCID: PMC9983143. Epub 2023/03/07. eng.
[104] Krishnadas N, Huang K, Schultz SA, Doré V, Bourgeat P, Goh AMY, et al. Visually identified Tau 18F-MK6240 PET patterns in symptomatic Alzheimer's Disease. J Alzheimers Dis 2022;88(4):1627–37. PubMed PMID: 35811517. PMCID: PMC9484111. Epub 2022/07/12. eng.
[105] Tissot C, Servaes S, Lussier FZ, Ferrari-Souza JP, Therriault J, Ferreira PCL, et al. The Association of Age-Related and off-target retention with longitudinal quantification of [(18)F]MK6240 tau PET in target regions. J Nucl Med 2023 Mar;64(3):452–9. PubMed PMID: 36396455. PMCID: PMC10071794. Epub 2022/11/18. eng.
[106] Rowe CC, Doré V, Krishnadas N, Burnham S, Lamb F, Mulligan R, et al. Tau imaging with ^{18}F-MK6240 across the Alzheimer's Disease spectrum. medRxiv 2022. 2022.02.13.22270894.
[107] Bauer T, Brendel M, Zaganjori M, Bernhardt AM, Jäck A, Stöcklein S, et al. Pragmatic algorithm for visual assessment of 4-Repeat tauopathies in [(18)F]PI-2620 PET Scans. Neuroimage 2025 Feb 1;306:121001. PubMed PMID: 39798829. Epub 20250109. eng.
[108] Smith R, Hägerström D, Pawlik D, Klein G, Jögi J, Ohlsson T, et al. Clinical utility of Tau Positron emission tomography in the diagnostic workup of patients with cognitive symptoms. JAMA Neurol 2023 Jul 1;80(7):749–56. PubMed PMID: 37213093. PMCID: PMC10203972 Alzheimer Foundation (AF-939981), Regionalt Forskningsstöd (2021-1013), the Kockska Foundation, and the Swedish federal government under the ALF agreement (2020-YF0020), and non-financial support from Roche during the conduct of the study and speaker fees from Roche outside the submitted work. Dr Pawlik reported grants from Swedish government under the ALF agreement during the conduct of the study. Dr Klein reported being a full-time employee and stakeholder of F. Hoffmann-La Roche during the conduct of the study. Dr Hansson reported non-financial support from Roche during the conduct of the study (RO948) and consultant fees from Biogen, Eisai, and BioArtic outside the submitted work. No other disclosures were reported. Epub 2023/05/22. eng.
[109] Sperling RA, Donohue MC, Rissman RA, Johnson KA, Rentz DM, Grill JD, et al. Amyloid and tau prediction of cognitive and functional decline in unimpaired older individuals: longitudinal data from the A4 and LEARN studies. J Prev Alzheimers Dis 2024;11(4):802–13. PubMed PMID: 39044488. PMCID: PMC11266444. eng.
[110] Makaretz SJ, Quimby M, Collins J, Makris N, McGinnis S, Schultz A, et al. Flortaucipir tau PET imaging in semantic variant primary progressive aphasia. J Neurol Neurosurg Psychiatry 2018 Oct;89(10):1024–31. PubMed PMID: 28986472. PMCID: PMC5964045. Epub 20171006. eng.
[111] Schaeverbeke J, Celen S, Cornelis J, Ronisz A, Serdons K, Van Laere K, et al. Binding of [(18)F]AV1451 in post mortem brain slices of semantic variant primary progressive aphasia patients. Eur J Nucl Med Mol Imaging 2020 Jul;47(8):1949–60. PubMed PMID: 31848674. PMCID: PMC7300115. Epub 20191218. eng.
[112] Shcherbinin S, Morris A, Higgins IA, Tunali I, Lu M, Deveau C, et al. Tau as a diagnostic instrument in clinical trials to predict amyloid in Alzheimer's disease. Alzheimer's Dement 2023 Jul-Sep;9(3):e12415. PubMed PMID: 37600216. PMCID: PMC10432878. Epub 20230816. eng.
[113] Hammes J, Bischof GN, Bohn KP, Onur Ö, Schneider A, Fliessbach K, et al. One-stop shop: (18)F-Flortaucipir PET differentiates amyloid-positive and -Negative forms of neurodegenerative diseases. J Nucl Med 2021 Feb;62(2):240–6. PubMed PMID: 32620704. Epub 20200703. eng.
[114] Mattay VS, Fotenos AF, Ganley CJ, Marzella L. Brain tau imaging: Food and drug administration approval of ^{18}F-Flortaucipir Injection. J Nucl Med 2020;61(10):1411–2.
[115] Coomans EM, de Koning LA, Rikken RM, Verfaillie SCJ, Visser D, den Braber A, et al. Performance of a [(18)F]Flortaucipir PET visual read method across the alzheimer disease continuum and in dementia with lewy bodies. Neurology 2023 Nov 7;101(19):e1850–62. PubMed PMID: 37748892. PMCID: PMC10663007. Epub 20230925. eng.
[116] Ossenkoppele R, Pichet Binette A, Groot C, Smith R, Strandberg O, Palmqvist S, et al. Amyloid and tau PET-positive cognitively unimpaired individuals are at high risk for future cognitive decline. Nat Med 2022 2022/11/01;28(11):2381–7.
[117] Josephs KA, Tosakulwong N, Weigand SD, Graff-Radford J, Schwarz CG, Senjem ML, et al. Flortaucipir PET uncovers relationships between tau and amyloid-β in primary age-related tauopathy and Alzheimer's disease. Sci Transl Med 2024 Jul 24;16(757). eado8076. PubMed PMID: 39047115. PMCID: PMC11423951. Epub 2024/07/26. eng.
[118] Fleisher AS, Pontecorvo MJ, Devous MD, Sr Lu M, Arora AK, Truocchio SP, et al. Positron emission tomography imaging with [18F]flortaucipir and postmortem assessment of alzheimer disease neuropathologic changes. JAMA Neurol 2020;77(7):829–39.
[119] Sonni I, Lesman Segev OH, Baker SL, Iaccarino L, Korman D, Rabinovici GD, et al. Evaluation of a visual interpretation method for tau-PET with (18)F-flortaucipir. Alzheimer's Dement 2020;12(1):e12133. PubMed PMID: 33313377. PMCID: PMC7699207. Epub 2020/12/15. eng.
[120] Mathoux G, Boccalini C, Peretti DE, Arnone A, Ribaldi F, Scheffler M, et al. A comparison of visual assessment and semi-quantification for the diagnostic and prognostic use of [(18)F]flortaucipir PET in a memory clinic cohort. Eur J Nucl Med Mol Imaging 2024 May;51(6):1639–50. PubMed PMID: 38182839. PMCID: PMC11041710. Epub 2024/01/06. eng.
[121] Seibyl JP, DuBois JM, Racine A, Collins J, Guo Q, Wooten D, et al. A visual interpretation Algorithm for assessing brain tauopathy with (18)F-MK-6240 PET. J Nucl Med 2023 Mar;64(3):444–51. PubMed PMID: 36175137. PMCID: PMC10071795. Epub 2022/09/30. eng.
[122] Smith R, Schöll M, Leuzy A, Jögi J, Ohlsson T, Strandberg O, et al. Head-to-head comparison of tau positron emission tomography tracers [18F]flortaucipir and [18F]RO948. Eur J Nucl Med Mol Imag 2020;47(2):342–54. 2020/02/01.
[123] Tonietto M, Sotolongo-Grau O, Roé-Vellvé N, Bullich S, Tartari JP, Sanabria Á, et al. Head-to-head comparison of tau PET tracers [18F]PI-2620 and [18F]RO948 in non-demented individuals with brain amyloid deposition: the TAU-PET FACEHBI cohort. Alzheimers Res Ther 2024 2024/11/28;16(1):257.
[124] Lois C, Gonzalez I, Johnson KA, Price JC. PET imaging of tau protein targets: a methodology perspective. Brain Imaging Behav 2019 Apr;13(2):333–44. PubMed PMID: 29497982. PMCID: PMC6119534.
[125] Bollack A, Pemberton HG, Collij LE, Markiewicz P, Cash DM, Farrar G, et al. Longitudinal amyloid and tau PET imaging in Alzheimer's disease: a systematic review of methodologies and factors affecting quantification. Alzheimer's Dement 2023 Nov;19(11):5232–52. PubMed PMID: 37303269. Epub 20230612.
[126] Baker SL, Maass A, Jagust WJ. Considerations and code for partial volume correcting [(18)F]-AV-1451 tau PET data. Data Brief 2017 Dec;15:648–57. PubMed PMID: 29124088. PMCID: PMC5671473. Epub 2017/11/11.
[127] Young CB, Landau SM, Harrison TM, Poston KL, Mormino EC. Adni. Influence of common reference regions on regional tau patterns in cross-sectional and longitudinal [(18)F]-AV-1451 PET data. Neuroimage 2021 Nov;243:118553. PubMed PMID: 34487825. PMCID: PMC8785682. Epub 20210903.
[128] Southekal S, Devous Sr MD, Kennedy I, Navitsky M, Lu M, Joshi AD, et al. Flortaucipir F 18 quantitation using parametric estimation of reference signal intensity. J Nucl Med 2018 Jun;59(6):944–51. PubMed PMID: 29191858. Epub 2017/12/02.
[129] Moscoso A, Grothe MJ, Scholl M. Alzheimer's Disease Neuroimaging I. Reduced [(18)F]flortaucipir retention in white matter hyperintensities compared to normal-appearing white matter. Eur J Nucl Med Mol Imaging 2021 Jan 21. PubMed PMID: 33475761. Epub 2021/01/22.
[130] Pontecorvo MJ, Devous MD, Kennedy I, Navitsky M, Lu M, Galante N, et al. A multicentre longitudinal study of flortaucipir (18F) in normal ageing, mild cognitive impairment and Alzheimer's disease dementia. Brain 2019 Jun 1;142(6):1723–35. PubMed PMID: 31009046. PMCID: PMC6536847. Epub 2019/04/23. eng.
[131] Jack Jr CR, Wiste HJ, Schwarz CG, Lowe VJ, Senjem ML, Vemuri P, et al. Longitudinal tau PET in ageing and Alzheimer's disease. Brain 2018 May 1;141(5):1517–28. PubMed PMID: 29538647. PMCID: PMC5917767.
[132] Jack Jr CR, Wiste HJ, Weigand SD, Therneau TM, Lowe VJ, Knopman DS, et al. Defining imaging biomarker cut points for brain aging and Alzheimer's disease. Alzheimer's Dement 2017 Mar;13(3):205–16. PubMed PMID: 27697430. PMCID: PMC5344738. Epub 2016/10/30.
[133] Villemagne VL, Leuzy A, Bohorquez SS, Bullich S, Shimada H, Rowe CC, et al. CenTauR: toward a universal scale and masks for standardizing tau imaging studies. Alzheimer's Dement 2023 Jul-Sep;15(3):e12454. PubMed PMID: 37424964. PMCID: PMC10326476. Epub 20230707.
[134] Biel D, Brendel M, Rubinski A, Buerger K, Janowitz D, Dichgans M, et al. Tau-PET and in vivo Braak-staging as prognostic markers of future cognitive decline in cognitively normal to demented individuals. Alzheimers Res Ther 2021 Aug 12;13(1):137. PubMed PMID: 34384484. PMCID: PMC8361801. Epub 20210812.
[135] Whittington A, Gunn RN. Alzheimer's disease neuroimaging I. Tau(IQ): a canonical image based algorithm to quantify tau PET scans. J Nucl Med 2021 Sep 1;62(9):1292–300. PubMed PMID: 33517326. PMCID: PMC8882899. Epub 20210130.
[136] Schafer A, Mormino EC, Kuhl E. Network diffusion modeling explains longitudinal tau PET data. Front Neurosci 2020;14:566876. PubMed PMID: 33424532. PMCID: PMC7785976. Epub 20201223.
[137] Franzmeier N, Dewenter A, Frontzkowski L, Dichgans M, Rubinski A, Neitzel J, et al. Patient-centered connectivity-based prediction of tau pathology spread in Alzheimer's disease. Sci Adv 2020 Nov;6(48). PubMed PMID: 33246962. PMCID: PMC7695466. Epub 20201127.
[138] Doering S, McCullough A, Gordon BA, Chen CD, McKay N, Hobbs D, et al. Deconstructing pathological tau by biological process in early stages of Alzheimer disease: a method for quantifying tau spatial spread in neuroimaging. EBioMedicine 2024 May;103:105080. PubMed PMID: 38552342. PMCID: PMC10995809. Epub 20240328.
[139] Coomans EM, van Tol B, Groot C, Smith R, Palmqvist S, Stomrud E, et al. Quantitation of PET spatial extent as a potential adjunct to visual interpretation of [(18)F]flortaucipir imaging: TAU-SPEX. Eur J Nucl Med Mol Imaging 2025 Jun 7. PubMed PMID: 40481862. Epub 20250607. eng.
[140] Franzmeier N, Dewenter A, Frontzkowski L, Dichgans M, Rubinski A, Neitzel J, et al. Patient-centered connectivity-based prediction of tau pathology spread in Alzheimer's disease. Sci Adv 2020;6(48). eabd1327.
[141] Doering E, Hoenig MC, Giehl K, Dzialas V, Andrassy G, Bader A, et al. "Fill States": PET-derived markers of the spatial extent of alzheimer disease pathology. Radiology 2025 Mar;314(3):e241482. PubMed PMID: 40131110. PMCID: PMC11950890.
[142] Harrison TM, Ward TJ, Murphy A, Baker SL, Dominguez PA, Koeppe R, et al. Optimizing quantification of MK6240 tau PET in unimpaired older adults. Neuroimage 2023 Jan;265:119761. PubMed PMID: 36455762. PMCID: PMC9957642. Epub 20221128.

[143] Costoya-Sanchez A, Moscoso A, Sobrino T, Ruibal A, Grothe MJ, Scholl M, et al. Partial volume correction in longitudinal tau PET studies: is it really needed? Neuroimage 2024 Apr 1;289:120537. PubMed PMID: 38367651. Epub 20240215.
[144] Leuzy A, Raket LL, Villemagne VL, Klein G, Tonietto M, Olafson E, et al. Harmonizing tau positron emission tomography in Alzheimer's disease: the CenTauR scale and the joint propagation model. Alzheimer's Dement 2024 Sep;20 (9):5833–48. PubMed PMID: 39041435. PMCID: PMC11497758. Epub 20240723.
[145] Povala G, Bauer-Negrini G, Bellaver B, Lussier FZ, Amaral L, Ferreira PC, et al. Creating universal tau PET Scale (Uniτ) parametric images–the HEAD study. Alzheimer's & Dementia 2024;20:e094123.
[146] Josephs KA, Martin PR, Botha H, Schwarz CG, Duffy JR, Clark HM, et al. [18F] AV-1451 tau-PET and primary progressive aphasia. Ann Neurol 2018;83(3): 599–611.
[147] Tsai RM, Bejanin A, Lesman-Segev O, LaJoie R, Visani A, Bourakova V, et al. (18) F-flortaucipir (AV-1451) tau PET in frontotemporal dementia syndromes. Alzheimers Res Ther 2019 Jan 31;11(1):13. PubMed PMID: 30704514. PMCID: PMC6357510. Epub 2019/02/02. eng.

Matthias Brendel[a,b,c,d,e,*], Phillip H. Kuo[f], Joachim Brumberg[g,h], Vincent Doré[i,j], Alexander Drzezga[k,l,m], Valentina Garibotto[n,o,p], Antoine Leuzy[q], Gregory Mathoux[n], Philipp T. Meyer[g,h], Alexis Moscoso[q,r], Rik Ossenkoppele[s,t], Tharick Pascoal[u,v], Ruben Smith[s,w], John Seibyl[x], Elsmarieke van de Giessen[y], Donatienne Van Weehaeghe[z], Marie R. Vermeiren[aa], Victor L. Villemagne[j,u,ab], Shadi A. Esfahani[ac,ad], Henryk Barthel[ae,af] the EANM Neuroimaging Committee

[a] *Department of Nuclear Medicine, LMU University Hospital, LMU Munich, Munich, Germany*
[b] *Munich Cluster for Systems Neurology (SyNergy), Munich, Germany*
[c] *German Center for Neurodegenerative Diseases (DZNE) Munich, Munich, Germany*
[d] *German Cancer Consortium (DKTK), Partner Site Munich, A Partnership Between the DKFZ Heidelberg and the University Hospital of the LMU, Munich, Germany*
[e] *Bavarian Cancer Research Center (BZKF), Partner Site Munich, Munich, Germany*
[f] *City of Hope National Medical Center, Department of Radiology, Los Angeles, USA*
[g] *Department of Nuclear Medicine, Medical Center-University of Freiburg, Freiburg, Germany*
[h] *Faculty of Medicine, University of Freiburg, Freiburg, Germany*
[i] *Australian E-Health Research Centre, CSIRO, Parkville, Australia*
[j] *Department of Molecular Imaging and Therapy, Austin Health, Heidelberg, Australia*
[k] *Department of Nuclear Medicine University Hospital Cologne, Köln, Germany*
[l] *German Center for Neurodegenerative Diseases (DZNE), Bonn, Germany*
[m] *Institute of Neuroscience and Medicine-Molecular Organization of the Brain (INM-2) Forschungszentrum Jülich, Jülich, Germany*
[n] *Division of Nuclear Medicine and Molecular Imaging, Geneva University Hospitals, Geneva, Switzerland*
[o] *4NIMTLab, Faculty of Medicine, University of Geneva, Geneva, Switzerland*
[p] *5Center for Biomedical Imaging (CIBM), Geneva, Switzerland*
[q] *ZRO Imaging, Santiago de Compostela, Spain*
[r] *Nuclear Medicine Department and Molecular Imaging Group, Instituto de Investigación Sanitaria de Santiago de Compostela, Travesía da Choupana S/N, Santiago de Compostela, Spain*
[s] *Clinical Memory Research Unit, Department of Clinical Sciences Malmö, Lund University, Lund, Sweden*
[t] *VU University Medical Center, Department of Neurology and Alzheimer Center, Amsterdam Neuroscience, Amsterdam, the Netherlands*
[u] *Department of Psychiatry, School of Medicine, University of Pittsburgh, Pittsburgh, PA, USA*
[v] *Department of Neurology, School of Medicine, University of Pittsburgh, Pittsburgh, PA, USA*
[w] *Memory Clinic, Skåne University Hospital, Malmö, Sweden*
[x] *Institute for Neurodegenerative Disorders, New Haven, CT, USA*
[y] *Department of Radiology and Nuclear Medicine, Amsterdam UMC, Location Vrije Universiteit, the Netherlands*
[z] *Department of Radiology and Nuclear Medicine, Ghent University Hospital, Ghent, Belgium*
[aa] *Department of Neurology, Erasmus University Medical Center, Rotterdam, the Netherlands*
[ab] *Alzheimer's Disease Research Center, University of Pittsburgh, Pittsburgh, PA, USA*
[ac] *Division of Nuclear Medicine and Molecular Imaging, Department of Radiology, Massachusetts General Hospital, Harvard Medical School, Boston, MA, USA*
[ad] *Center for Precision Imaging, Division of Nuclear Medicine and Molecular Imaging, Department of Radiology, Massachusetts General Hospital, Boston, MA, USA*
[ae] *Department of Nuclear Medicine, University of Leipzig, Leipzig, Germany*
[af] *Clinic for Nuclear Medicine, City Hospital Dessau, Dessau, Germany*

[*] Corresponding author. LMU Hospital, Marchioninistrasse 15, 81377, Munich, Germany.
E-mail address: Matthias.Brendel@med.uni-muenchen.de (M. Brendel).